POLITECNICO DI MILANO

FACOLTÀ DI INGEGNERIA DEI SISTEMI
Corso di Laurea Magistrale in Ingegneria Biomedica

Multimodal Navigation System for Brain Mapping notification and Brain Shift estimation

Relatore:
Ing. Elena DE MOMI

Correlatori:
Dott.ssa Chiara CABORNI
Dott. Francesco CARDINALE

Tesi di Laurea Magistrale di:
Paolo BASSANINI
Matricola 765152

Anno Accademico 2011-2012

Multimodal Navigation System for Brain Mapping notification and Brain Shift estimation

Paolo Bassanini

April 22, 2013

Multimodal navigation system for brain mapping notification and brain shift estimation

Paolo Bassanini

Acknowledgements

This thesis is the result of my work that took place at Politecnico di Milano, Department of Electronic, Information and Bioengineering (DEIB) at NearLab from March 2012 till April 2013 thanks to the continuos support I had from Chiara Caborni and Elena De Momi at the laboratory. The project started and took its actual form at Niguarda Hospital in Milano thanks to MD Francesco Cardinale, neurosurgeon. Medtronic has been involved represented by Daniele Marinucci (Navigation Specialist at Medtronic Italia), great technical support in particular during the development of the code came from Timothy Schaewe PhD and Holton Leslie PhD from Medtronic Research (US). For the feasibility study a great thanks goes to MD Giuseppe Casaceli, neurosurgeon at Niguarda Hospital who collected most of the points used for the brain shift analysis and to the other surgeons that allowed the experiments: Massimo Cossu, MD and Giorgio Lo Russo, MD.

Abstract

The necessity of localization of intracranial targets such as tumors or lesions during surgical interventions has been perceived since the beginning of the XX century. In 1949 the stereotactic system was developed by Leksell. This system (still used today for certain neurosurgical interventions, such as biopsies or depth electrodes insertion) is fixed to the patient head and is based on the use of a tridimensional coordinates system for the precise localization. This system has a cumbersome structure that the patient must wear preoperatively during imaging. There has been thus the necessity to have tools more handy and flexible such as neuronavigators which continuously monitor the position of the patient head and the position of the surgical tool used during the operation. A registration procedure with the preoperative images is required.

Among the others, commercial navigation systems currently used for neurosurgery are the StealthStation (Medtronic, Minneapolis, US) and the Vector Vision (BrainLab, Feldkirchen, Germany). Some researchers have integrated the Medtronic neuronavigator and the open-source visualization environment 3D Slicer (`www.slicer.org`). 3D Slicer was used for monitoring and limiting the surgical robot working area [14]. In other studies the navigation software has been adapted for adding intraoperative annotation and sound feedback [20]. The integration of another commercial system (BrainLab) with the open-source software Bioimage Suite (`www.bioimagesuite.com`, an integrated medical image analysis suite) had the finality to improve the visualization environment used for intraoperative navigation [23, 31].

One of the main limitation that affect modern neuronavigation accuracy is brain shift: a phenomena that de facto invalidates the hypothesis of the equivalence between the surgical reality and the diagnostic preoperative images. It was demonstrated that the phenomena can reduce the accuracy of the navigation up to 2.5 cm [7] and that the main brain shift occurs in the gravity direction [27]. Brain shift is due to to the leakage of cerebro spinal fluid (CSF) with consequent intracranial pressure drop and happens mainly after the dura mater opening. Some authors demonstrated that there is not a direct correlation between the entity of the brain shift and the dimensions of the craniotomy, the patient orientation and the usage of hyperosmotic drugs such as mannitol. Nevertheless those factors are for sure concauses of the phenomena.

This thesis work is aimed at providing the surgeon with a navigation system that would allow a more complete visualization with respect to the commercial systems. In particular the aim has been the integration of an existing navigation system inside an open source software for the analysis and the visualization of preoperative data. Specific thesis objectives pursued are:

- implementing an intraoperative annotation functionality;
- collection of cortex fiducials during the operation to estimate the brain shift.

3D Slicer [9] is a software platform for the analysis and visualization of medical images and for research in image guided therapy. Features include: support for

many modalities, including: Magnetic Resonance Imaging (MRI), Computed Tomography (CT), UltraSound (US), Diffusion Tensor Imaging (DTI); flexible display capabilities with a variety of predefined layout for slice reformats and 3D views; automated and interactive segmentation tools; surface reconstruction from image data; extensible & scriptable development platform (C++/Python).

The Medtronic navigator (StealthStation TREON Plus) was integrated in 3DSlicer through a Windows client that accesses data from the navigator and send processed data to 3DSlicer. The software make use of proprietary (StealthLink) and open-source (OpenIGTLink[31]) protocols for the communications over the hospital network. The possibility to acquire intraoperative points through the pointer and visualize them in the 3D Slicer scene was implemented. The feature was developed for two purposes:

1. visualization of cortical electrostimulated points on the Slicer scene, allowing the user to set the annotation description and the color;

2. analyzing the shift of cortical points caused by brain shift, through the annotation of the same cortical features at different time during surgery, in order to analyze the displacement of those features.

Brain shift was studied analyzing the evolution of cortical points in 7 resective surgeries performed at "Claudio Munari" centre for epilepsy surgery at Niguarda Cà Granda Hospital, Milan. The experimental protocol consisted in the following phases:

- acquisition of the gravity vector direction with respect to the patient;
- acquisition of the performed craniotomy border;
- acquisition of 3-7 cortical points in different phases of the intervention.

Shift vectors were defined as the difference between corresponding points acquired at different time frame. They represent the direction and the entity of the shift occurred for each cortical point. Craniotomy plane was defined as the plane approximating the points of the craniotomy border acquired; the brain inward direction was defined as the vector normal to the craniotomy plane; the craniotomy orientation was defined as the angle between the brain inward direction and gravity vector. Data acquired were processed with Matlab® and the Visualization ToolKit (VTK). The following quantitates were estimated:

1. module and direction of the shift vectors;

2. correlation between shift vectors, the craniotomy opening and the craniotomy orientation during surgery.

Patients underwent a median shift of 5 mm (maximum 7 mm and minimum 2.6 mm). Three patients with a brain shift lower than the measured system accuracy (4,21 mm) were discarded.

The median angle between shift vectors and the gravity vector results 34°, and the median angle between shift vectors and the inward brain direction results 50°. The main direction of brain shift is thus gravity.

A deeper analysis was performed on the discarded patients leading to the results that the non feasibility of those data is due to one the following reasons:

- brain shift occurred in cortical regions in which none or few points were acquired;
- brain shift occurred in opposite directions at different cortical regions.

It was not found a correlation of the brain shift with the extent of the craniotomy, but a correlation with the craniotomy orientation was found differently from the state of the art [27].

In conclusion, this thesis project reached its first objective providing surgeons at the centre of Niguarda Hospital with a navigation system additional to the one currently used, with improved functionalities and more features. These functionalities allowed the realization of a preliminary study of the complex phenomena of brain shift. Results of this study are in partial agreement with the state of art but an increased number of patient is necessary.

In the future acquisition methodologies can be improved and the sample size could surely increase. The work can be directed to several ways: the system optimization, its integration with surgical robotic systems, the usage of the systems for clinical studies of different nature.

Key-words: Image guided surgery, neuronavigation, 3D Slicer, Medtronic StealthStation, Brain Shift.

Sommario

La necessità di localizzare target intracranici quali tumori o lesioni durante interventi chirurgici è stata percepita fin dagli inizi del XX secolo. Nel 1949 il sistema stereotassico fu sviluppato da Leksell. Questo sistema (tutt'oggi utilizzato per alcuni interventi chirurgici, come biopsie o inserimento di elettrodi di profondità) è fissato alla testa del paziente ed è basato sull'uso di un sistema tridimensionale di coordinate per la precisa localizzazione. Questo sistema ha una struttura ingombrante che il paziente deve indossare prima dell'intervento per sottoporsi all'esame radiologico. C'è stata dunque la necessità di avere strumenti più maneggevoli e flessibili come i neuronavigatori i quali monitorano continuamente la posizione della testa del paziente e la posizione di uno strumento chirurgico utilizzato durante l'operazione. Una procedura di registrazione con le immagini preoperatorie è richiesta.

Tra gli altri, i sistemi di navigazione correntemente utilizzati in neurochirurgia sono: StealthStation (Medtronic, Minneapolis, USA) e Vector Vision (BrainLab, Feldkirchen, Germania). Alcuni ricercatori hanno integrato il neuronavigatore Medtronic e l'ambiente open-source di visualizzazione 3D Slicer (`www.slicer.org`). 3D Slicer è stato utilizzato per il monitoraggio e la limitazione dell'area di lavoro di un robot chirurgico [14]. In altri studi il software di navigazione è stato adattato per aggiungere funzionalità di annotazione intraoperatoria e feedback sonoro [20]. L'integrazione di un altro sistema commerciale (BrainLab) con il software open-source Bioimage Suite (`www.bioimagesuite.com`, un ambiente integrato per analisi di immagini mediche) ha avuto la finalità di migliorare l'ambiente di visualizzazione utilizzato per la navigazione intraoperatoria [23, 31].

Una delle principali limitazioni che colpisce l'accuratezza dei moderni sistemi di neuronavigazione è il brain shift: un fenomeno che di fatto invalida l'ipotesi di equivalenza tra la realtà operatoria e le immagini diagnostiche preoperatorie. E' stato dimostrato che il fenomeno può ridurre l'accuratezza della navigazione fino a 2,5 cm [7] e che il brain shift avviene principalmente in direzione della gravità [27]. Il brain shift è dovuto alla fuoriuscita di liquido cerebrospinale con conseguente caduta di pressione intracranica ed inizia a verificarsi dopo l'apertura durale. Alcuni autori hanno dimostrato che non c'è correlazione diretta tra l'entità del brain shift e le dimensioni della craniotomia, l'orientamento del paziente e l'uso di farmaci iperosmotici come il mannitolo. Tuttavia questi fattori sono senza dubbio concause del fenomeno.

Questo lavoro di tesi si propone di fornire al chirurgo un sistema di navigazione che possa consentire una visualizzazione più completa rispetto ai sistemi commerciali. In particolare l'obiettivo è stato l'integrazione di un sistema di navigazione esistente all'interno di un software open-source per l'analisi e la visualizzazione di dati preoperatori. Obiettivi specifici perseguiti sono stati:

- l'implementazione di un sistema di annotazione intraoperatoria;
- l'acquisizione di punti fiduciali corticali durante alcune operazioni per stimare il brain shift.

3D Slicer [9] è una piattaforma software per l'analisi e la visualizzazionedi immagini mediche e per ricerche nell'ambito della chirurgia guidata dalle immagini. Le sue caratteristiche includono: supporto per molte modalità di immagini diagnostiche tra cui: Risonanza Magnetica (RM), Tomagrafia Assiale Computerizzata (TAC), Ultrasuoni (US), Imaging con Tensore di Diffusione (DTI); possibiltà di visualizzazione flessibile con una varietà di formati predefiniti for la visualizzazione delle immagini bidimensionali dell'esame e dei modelli tri-dimensionali; strumenti per la segmentazione automatica e interattiva; ricostruzione di superfici dalle immagini; piattaforma di sviluppo estensibile (C++/Python).

Il navigatore Medtronic (StealthStation TREON Plus) è stato integrato in 3D Slicer attraverso un Windows client che accede ai dati del navigatore e invia i dati elaborati a 3DSlicer. Il software utilizza protocolli di comunicazione proprietari (StealthLink) e open-source (OpenIGTLink [31]) per la comunicazione all'inerno della rete dell'ospedale. E' stata inoltre implementata la possibilità di acqusisire punti intraoperatori attraverso il pointer e di visualizzarli in 3D Slicer. La funzione è stata sviluppata per due scopi:

1. visualizzazione di punti corticali stimolati elettricamente nella scene di Slicer, consentendo all'utente di impostare la descrizione e il colore dell'annotazione;
2. analizzare lo spostamento di punti corticali casusato dal brain shift, attraverso l'annotazione della stesso punto corticale in diverse fasi dell'intervento, per analizzare lo spostamento del punto.

Il brain shift è stato studiato analizzando l'evoluzione di punti corticali in 7 procedure di chirurgia resettiva effettuate al centro di chirurgia dell'epilessia "Claudio Munari" all'ospedale Niguarda Cà Granda di Milano. Il protocollo sperimentale è consistito nelle seguenti fasi:

- Acquisizione della direzione del vettore gravità rispetto al paziente;
- Acquisizione dei bordi della craniotomia effettuata;
- Acquisizione di 3-7 punti corticali in diverse fasi dell'intevento.

I vettori spostamento sono stati definiti come differenza tra punti corrispondenti acquisiti in tempi diversi, essi rappresentano la direzione e l'entità dello spostamento subito per ciascun punto corticale; il piano di craniotomia è stato definito come il piano approssimante i punti acquisiti del bordo della craniotomia, la direzione entrante nel cervello è stata definita come il vettore normale al piano di craniotomia; l'orientamento della craniotomia è stato definito come l'angolo tra la direzione entrante nel cervello e il vettore gravità. I dati acquisiti sono stati analizzati con Matlab® e il Visualization ToolKit (VTK). Le seguenti quantità sono state stimate:

1. modulo e direzione dei vettori spostamento;
2. correlazione tra i vettori spostamento, la craniotomia e il suo orientamento durante l'operazione.

I pazienti hanno subito un brain shift mediano di 5 mm (massimo 7 mm e minimo 2.6 mm). Tre pazienti con un brain shift minore dell'accuratezza del sistema misurata (4,21 mm) sono stati scartati.

L'angolo mediano tra i vettori spostamento e il vettore gravità è risultato 34°, e l'angolo mediano tra i vettori spostamento e la direzione interna al cervello è risultato 50°. La direzione principale di brain shift è perciò la gravità.

Un'analisi approfondita effettuata sui pazienti scartati ha portato al risultato che la non affidabilità di tali analisi è dovuta a una delle seguenti ragioni:

- il brain shift è avvenuto in regioni corticali in cui nessuno o solo pochi punti sono stata acquisiti;
- il brain shift è avvenuto in direzioni opposte per diverse regioni corticali.

Non è stata trovata correlazione tra brain shift e l'estensione della craniotomia, ma una correlazione con l'orientamento della stessa è stato trovato a differenza delle stato dell'arte [27].

In conclusione, il progetto di tesi ha raggiunto il suo primo obiettivo fornendo ai chirurghi del centro dell'ospedale Niguarda un sistema di navigazione addizionale a quello correntemente in uso, con funzionalità aggiuntive. Queste funzionalità hanno consentito la realizzazione di uno studio preliminare del complesso fenomeno del brain shift. I risultati di questo studio sono in buona parte in accordo con lo stato dell'arte ma un numero maggiore di pazienti sarebbe necessario. Nel futuro i metodi di acquisizione potranno essere migliorati e il campione di dati potrà aumentare.

Il lavoro potrà essere continuato in diversi modi: l'ottimizzazione del sistema, la sua integrazione con sistemi di chirurgia robotica, l'uso del sistema per studi clinici di diversa natura.

Parole chiave: Chirurgia guidata dalle immagini, neuronavigazione, 3D Slicer, StealthStation, Brain Shift.

Contents

List of Figures

List of Tables

Chapter 1

Introduction

1.1 Navigation in neurosurgery

Since the beginning of modern neurosurgery at the end of the nineteenth century, neurosurgical progress has been intimately related to improvements in intraoperative localization of surgical target [12]. The knowledge of spatial relationships of lesions inside the cranium and the development of atraumatic approaches contributed essentially to reduced mortality and morbidity of neurosurgical interventions. Localization encompasses two aspects:

- where in the cranium the lesion or functional area must be assumed to be (pre-operative localization);
- how to find this lesion or area during operation (intra-operative localization).

At the beginning of the last century, the topic of diagnostic localization of lesions could be understood only by analyzing the neurologic symptoms of the patient, without the possibility of referring to radiologic images. The first imaging technique, introduced in 1918, was the visualization of the ventricles by direct injection of air and later of contrast medium into the ventricles or cisterna magna. From the shape and kind of ventricular displacement, lesions close to the midline structures could be detected [6]. Later, in 1927, angiography was described by Egas Moniz [1]. This technique allowed localization of intracranial lesions either directly by visualization of the pathologic vessels or indirectly by associating the lesion with a lobe, depending on the characteristic frontal, temporal, or occipital displacement of the intracerebral arteries. Direct visualization of the cerebral tissue was not possible before CT was introduced by Hounsfield in 1973.

For intraoperative target localization the first system has been developed by Lars Leksell in 1949: the frame based stereotactic system (Figure 1.1). It is a form of surgical intervention which makes use of a three-dimensional coordinate system to locate targets inside the brain and to guide ablation, biopsy,

lesion, injection, stimulation, implantation, etc. The usage of those systems require the attachment of an uncomfortable frame to an awake patient's head for preoperative imaging, they also limit the surgical positioning and exposure.

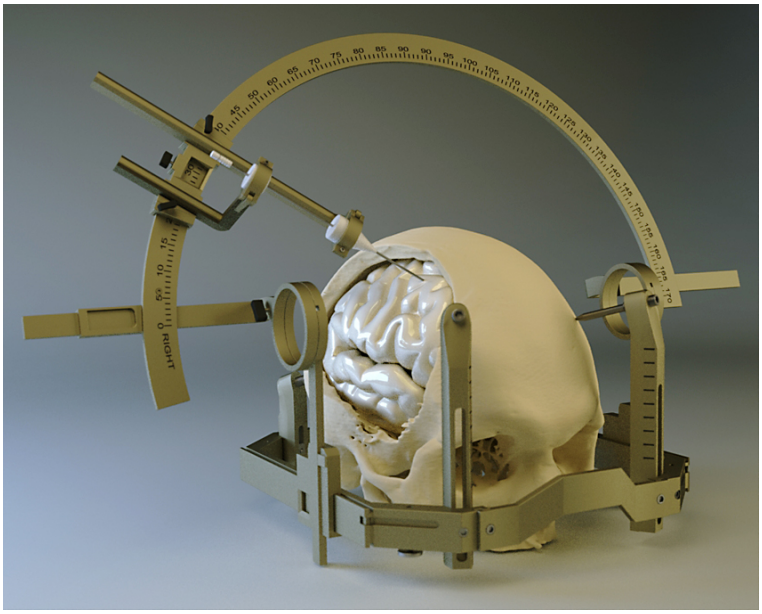

Figure 1.1: Stereotactic frame, first developed by Lars Leksell in 1949.

1.1.1 Frameless Navigation systems

The next evolutionary step of stereotactic surgery was neuronavigation. A neuronavigation system is composed by a localization system that tracks markers attached to surgical tools, a reference frame connected to patient head, a monitor, an image processing module (Figure 1.2). The image processing module loads, in the preoperative phase, different patient datasets and computes a three-dimensional (3D) model of the patient skin in order to make possible the registration procedure.

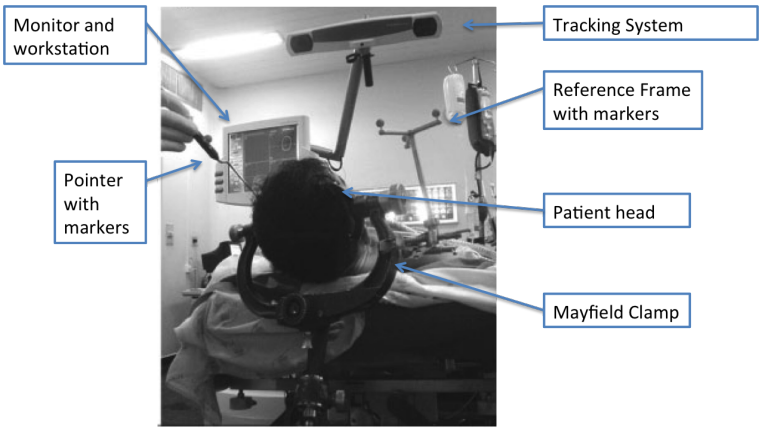

Figure 1.2: The components of a neuronavigation system are the monitor and workstation, the pointer, the reference frame and the tracking system. The Mayfield clamp is used to hold the patient head during registration and surgery. Thanks to the clamp the reference frame is connected to the patient during navigation.

The most-widely used localization systems utilize dual infrared cameras that track the position of a probe relative to a fixed reference frame (Figure 1.2). The main limitation of infrared-based systems is the need for maintaining a direct line of sight between the camera, the reference frame and the probe during navigation. Electromagnetic tracking systems are the major commercially available alternative to optical tracking systems. Electromagnetic-based navigation relies on the tracking of a probe within an electromagnetic field, created by a field generator in a fixed location: line of sight issues are completely obviated by the use of electromagnetic field-based tracking. Additionally, the electromagnetic navigational probes are smaller than the optical one, making use in catheter placement and under the microscope more straightforward [21]. Logistically, the main consideration with electromagnetic tracking is the relatively large size of the field generator and the need for its positioning close to the operative site. Furthermore, while concerns have been raised about the accuracy of electromagnetic field-based tracking systems given the presence of multiple ferromagnetic instruments in the operative field, evidences suggests that this is rarely a problem in the clinical environment [16].

The basic concept of neuronavigation are discussed in the following paragraphs.

Image registration To see the tip of a pointer in an image space, a relationship between the device space and the image space has to be established. This operation is called registration of the navigation device. Basically, a transformation matrix has to be calculated for mapping the coordinates of any point between the image and the device spaces. Registration techniques proposed are

mainly divided in two groups: Point to Point [32] and Surface registration [2]. In section 3.1.4 the methods provided by a commercial neuronavigation system will be described.

Navigational accuracy Electrode-based studies using pre and post-operative MRI suggested that modern frameless methods for localization yield positional accuracy within 2–3 mm during surgery, which is equivalent to the accuracy of frame-based stereotaxy[17]. The error inherent in frameless stereotactic navigation systems relates to the accuracy of probe tracking as well as the quality of preoperative images and the method of image to-patient registration [33]. Also clinical factors may diminish navigational accuracy, one of the main is the phenomena of **brain shift**. The problem will be analyzed in section 2.3 and a study of the phenomena will be part of this thesis work.

In the Table 1.1 the available commercial neuronavigation systems with their main features are shown.

		Tracking		**Registration**	
Company	**Country**	**Optic**	**EM**	**Point**	**Surface**
BrainLab	Germany	+	-	+	+
Compass	US	-	+	+	-
General Electric	US	-	+	+	+
Medtronic	US	+	+	+	+
Micromar	US	+	-	+	-
Sonowand	Norway	+	-	+	+
Stryker	US	+	-	+	+

Table 1.1: Commercial navigation system nowadays available with their main features: the tracking system (localizer) optical or electromagnetic, the registration type divided in Point to Point registration or Surface Registration, the last column of the table is the capability of the system to track any kind of surgical tools and not only the provided pointer.

In lesional epilepsies the intraoperative localization of the lesion and its location with respect the eloquent cortex that have to be preserved is essential for the neurosurgeon. The localization of eloquent areas is performed using Direct Electrical Stimulation (DES): a technique for inferring the function of brain areas in humans [4]. The working principle of the technique is the stimulation of the cortex with a bipolar or monopolar probe (Figure 1.3-left) and the registration of the consequent muscular response. It is surgical practice to roughly report the outcome of the stimulation (cortical structures to be avoided during surgical resection) on a brain model printed on paper (Figure 1.3-right).

Figure 1.3: Direct electrical cortex stimulation procedure (left) and manual annotation of the eloquent stimulated point (right).

1.2 Aim of the work

The aim of this thesis work was adding functionalities to a commercial neuronavigator used in epilepsy neurosurgey for:

- multimodal navigation: it will be possible to load a wide set of imaging modalities thanks to an open-source medical images visualization and processing software that will be adapted for navigation;
- enabling intraoperative annotations that are used for two purposes:
  1. allow the surgeon to place localized annotation of DES points (notification) on the brain 3D model;
  2. collection of cortex fiducials during the operation to estimate the brain shift.

Those functionalities were added through the integration of the Medtronic neuronavigation system into an external open-source software (3DSlicer 4, www.slicer.org, described in paragraph 3.2).

After the system integration was performed its accuracy was tested and finally it was performed a clinical study of one of the main factor that influence neuronavigators accuracy, the brain shift.

The idea behind this work is to take advantage of advanced image processing and visualization, which are not commercially available, from external research navigation software (e.g. 3D Slicer) and reliable surgical navigation features from an approved commercial navigation system (Medtronic), in order to investigate new technologies without interfering with the existing clinical procedure.

1.3 Outline of the thesis

The thesis is organized in 6 chapters.

- Chapter 2 gives some insight about the state of the art of the following areas: navigation system improvements and brain shift studies with possible solutions to the problem.
- A description of the materials and methods will be given in Chapter 3, together with the explanation of the experimental protocol of the clinical study.
- In Chapter 4 technical and clinical results will be described
- In Chapter 5 results will be discussed.
- In Chapter 6 some conclusion will be given and future perspective will be delineated.

Chapter 2

State of the art

2.1 Multimodal imaging in neuronavigation

Advances in Magnetic Resonance Imaging (MRI) have enabled the possibility of incorporating functional data into the neuronavigational datasets. In [15] it has been shown that the use of neuroimaging and functional navigation technologies may effectively lower the incidence of postoperative complications. There are currently two major types of functional datasets that are used for navigation: functional MRI (fMRI)[1] and diffusion tensor imaging (DTI)[2].

While fMRI may be used to highlight key cortical structures, DTI can be used for subcortical anatomy mapping. The main advantages are: better understanding of the relationship between a lesion to key subcortical fiber tracts allowing the avoidance of specific cortico-spinal tract during resection. DTI data can be incorporated into navigational datasets to allow surgeons to plan and revaluate surgical trajectories in three dimensions to minimize the risk of surgical injury to white matter tracts. In a randomized controlled trial of 238 patients comparing neuronavigation with or without DTI of the pyramidal tracts[34], it has been demonstrated that postoperative neurologic deficits were less frequent with the addition of DTI to the navigational dataset. Importantly, DTI can also be intraoperatively acquired to create updated positional information of key white matter tracts. As with other structures in the brain, the position of key fiber tracts changes over the course of an operation [28]. Nevertheless surgeons using DTI must keep in mind that subcortical stimulation (i.e DES) remains as the gold-standard for ascertaining the position of functional white matter tracts during surgery. A report by Zolal [35] in 36 patients who underwent subcortical white matter stimulation during brain tumor resection suggests that DTI provides a rough estimate of the true location of the

[1] fMRI is based on blood-oxygen level dependent changes in cortical regions that occur during specific tasks [3]. Regions of blood-oxygen level-dependent changes can be overlayed onto structural MR images to create volumes representing active cortical regions.

[2] DTI is based on the preferential diffusion of water in the direction of white matter tracts and it is a unique tool used by neurosurgeons.

cortico-spinal tract. Generally, a response can be elicited within 8mm of the location of the DTI-predicted cortico-spinal tract but distances of 0–15 mm for stimulation to tract distance have been reported [24]. Many factors such as tissue conductance, anatomical stimulation point (subcortical versus, internal capsule and brainstem) and stimulation parameters also affect the accuracy of subcortical white matter mapping. Consequently a combination of subcortical stimulation and DTI-informed navigation is likely to provide the most robust data for decision-making during the resection of lesions near key white matter tracts.

2.2 Commercial Neuronavigation systems Improvements

T. Haidegger [14] describes an integrated navigated robot system for skull base surgery (Figure 2.1). The robot (Neuromate, Renishaw-Mayfield SA, Nyon, Switzerland) cutting tool has been tracked by a neuronavigation system: Medtronic StealthStation® TREON (Medtronic Navigation, Louisville, CO, USA). Data coming from StealthStation® were accessed through StealthLink, a Medtronic provided research interface, and sent to 3D Slicer. In the planning phase, 3D Slicer have been used for model creation features to define the virtual fixture: a safety zone for avoiding critical structures, acting as virtual walls for the cutting tool attached to the robot. During the procedure, 3D Slicer provides a visualization of the surgical tool with respect to the virtual fixture and preoperative images.

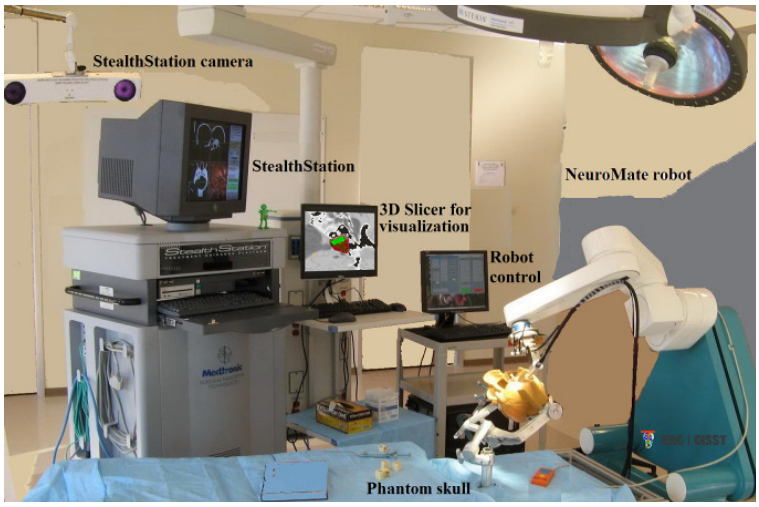

Figure 2.1: Robotic neurosurgery setup at the Johns Hopkins University. The system consists of a modified NeuroMate robot, a StealthStation® surgical navigation system and a PC station with the 3D Slicer software.

In [20] a modified version of the original navigation software was proposed, sound feedback and workflow tracking to improve the efficacy of brain tumor resection were added. A sound is produced whenever the surgical tool is operating far away from the planned resection area (Figure 2.2, left). On the right we can see the workflow tracking functionality: the blue dots are all the positions tracked by the system. Workflow feedback is meant to give the surgeon insight in the progress of tumor resection and it has the additional advantage of logging data of interest and giving a measure of brain shift. For the workflow feedback a separated software running on an external workstation has been developed. After patient selection and brain and tumor segmentation, a screen is presented to the user with an interactive slicer and 3D viewer based on high quality volume rendering (Figure 2.3). By enabling the button 'Track pointer' the system constantly inspects the log files produced by the adapted Stealthstation software to look for newly added instrument coordinates. Small soft spheres of about 1 mm in diameter are drawn at these coordinates in image space which become visible in the slider and 3D viewer. The spheres get a different label number based on the number of the log file. In this way separate instrument tracks can be distinguished with different text labels and color. Also, positions of electrical stimulations can be logged using different tracks.

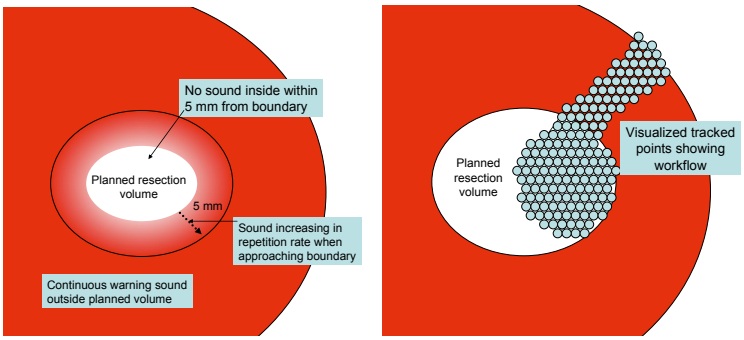

Figure 2.2: Principle of sound (left) and workflow feedback (right). Sound feedback: when the instrument tip is inside the tumor and more than 5 mm away from the boundary, no sound is given. When the tip approaches boundary, the sound repetition rate starts increasing until the boundary is reached. Then a continuous warning sound is produced. Workflow feedback: Instrument positions are continuously tracked and drawn on the planned resection volume. In this way the workflow can be followed in real-time, so it is easy to see non-resected parts or get an impression of brain shift.

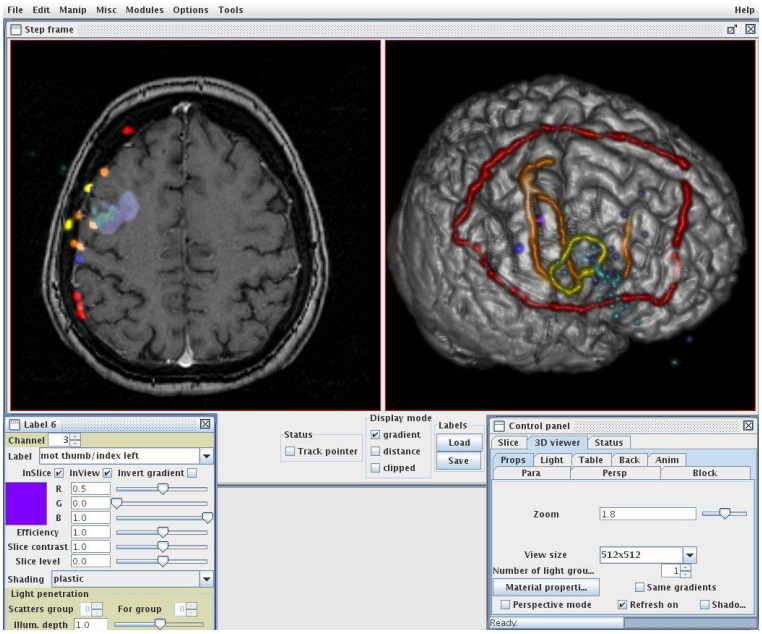

Figure 2.3: Intra-operative screen dump of workflow feedback software.

A different system was proposed by X. Papademetris [22]. He developed the client/server interface that provides data from the navigator (VectorVision, Cranial Navigation, BrainLAB AG, Feldkirchen, Germany), and communicates with an open-source software in which processing could be done (Bioimage suite software, Yale university [23]) and send processed data back to the navigator software. The developed client/server interface is part of the commercial version of the software and the system coupled with the open-source software has been tested twice in the operating room. The first time it has been tested in a electrode placement procedure and the second time in a surgical resection for epilepsy in which fMRI, Single Photon Emission Computed Tomography (SPECT), Magnetic Resonance Spectroscopy Imaging (MRSI) and 3D electrode localizations were made available to the surgeons within the Image Guided Surgery (IGS) environment. This was the first time they could navigate in real time with such integrated multi-modality data simultaneously displayed on the typical high resolution anatomical imaging.

In [31] it has been realized the integration of the VectorVision neruonavigation system in 3D Slicer using the OpenIGTLink protocol to transfer image and tracking data from the commercial system to 3D Slicer during a clinical case. The neuronavigator provides access to data using its internal VectorVision Link (VVLink) interface developed in the previous mentioned work. In order to establish communication between the two systems a bridge software was developed that receives images and tool positions from the BrainLAB system using VVLink, converts them into OpenIGTLink messages, and sends them

to 3D Slicer over the network. The integrated system has started to be tested in clinical cases to investigate new visualization techniques, which is not available in commercial systems (Figure 2.4). Despite the need for a 'double-hop' network connection, the real-time tool tracking has been maintained across the combined systems, demonstrating the feasibility of using a proxy system to translate from the proprietary protocol to OpenIGTLink, hence allowing for the interfacing of two unmodified systems simplifying the research task.

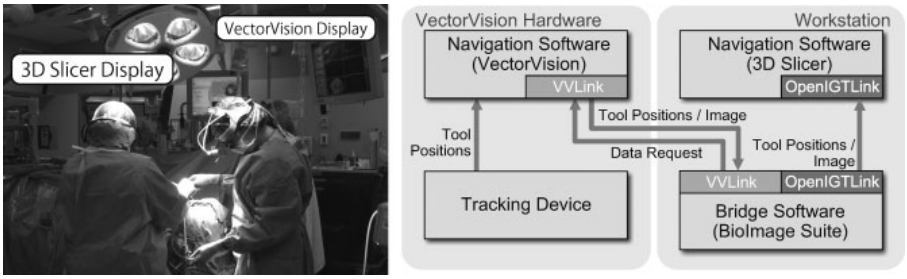

Figure 2.4: Overview (left) and system diagram (right) of VectorVision -3D Slicer integration in the operating room. VectorVision provides basic navigation features, including tool tracking and image display, while 3D Slicer provides advanced image processing. The surgeons can check both the VectorVision console and the 3D Slicer user interface on dedicated monitor during surgery.

2.3 Brain shift studies

As mentioned above, one of the main open issue regarding neuronavigation is the phenomenon of brain shift. The brain shift is the motion of cerebral structures occurring after the craniotomy. During craniotomy part of the skull is opened in order to access the brain. The cause of the brain shift is mainly the change of pressure due to loss of cerebrospinal fluid (CSF) occurring after craniotomy [7]. The result is a movement of up to 25 mm [7] (measured at the end of the surgery) of cerebral structures and a change of the brain volume. This can be clearly seen in Figure 2.5, by comparing the pre-operative and intra-operative MR-slice images of the brain.

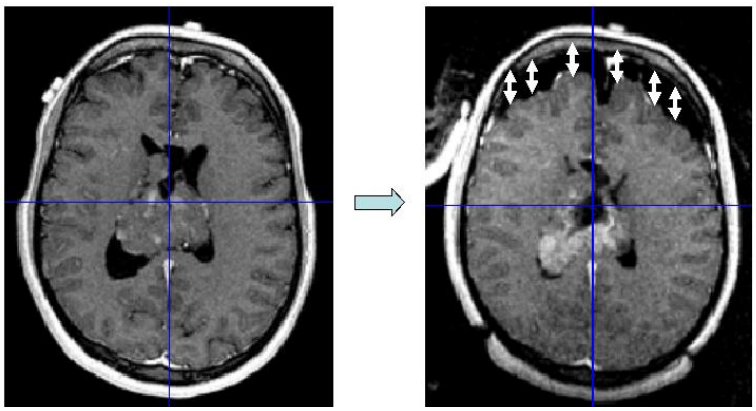

Figure 2.5: MR-slices pre-operative and intra-operative, showing the brain shift effect[7].

The phenomena negatively influence the navigation accuracy because de facto invalidates the hypothesis of the equivalence between the surgical reality and the diagnostic preoperative images. For the quantification of the intra-operative brain shift **photogrammetry** methods have been implemented [7]. A multi-camera system employed three USB2.0 progressive scan CCD cameras (model 2240-M/C of iDS, Figure 2.6, on the left): these cameras were arranged in a triangular form. A silicon replica of the brain was used and some points and lines were drown on the object. The employed material was soft, so that the brain replica could be deformed simulating the compression of cerebral structures. Relevant points on the brain surface are selected manually by the operator on a single image. The correspondent points in the other images are then automatically determined by a matching procedure based on epipolar constrained least square matching (LSM). The 3D coordinates of the selected points are then determined by forward ray intersection. The system has not been tested clinically yet but the results are promising because the software has demonstrated to feasibly track trajectories of 40 points in real-time (Figure 2.7). Nevertheless, performed experiments did not take into account that the surface available for tracking in a real surgical intervention is much more limited than the phantom used and also the deformation impressed to the phantom does not simulate a real brain shift effect. (Figure 2.6).

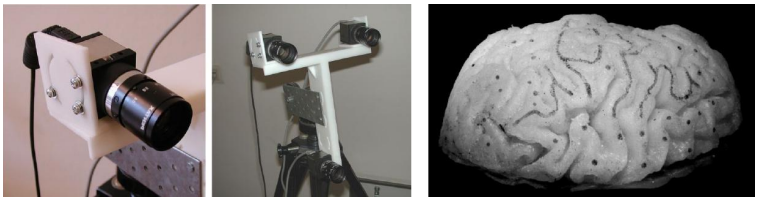

Figure 2.6: USB2.0 progressive scan CCD cameras 2240-M/C of iDS (left), silicon replica of a brain (right).

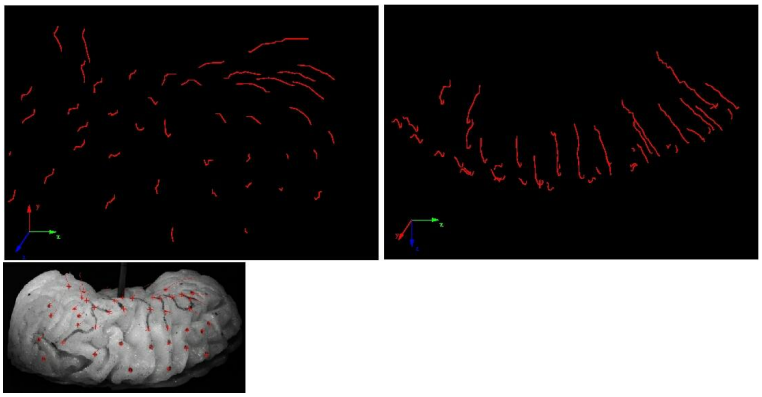

Figure 2.7: Two different 3D representations of the determined trajectories: frontal view (left), top view (right). Points tracked on the silicon replica of the brain (down).

A clinical brain shift quantitative study was performed by W. Roberts et.al, and described in [27]. A quantitative analysis of cortical displacement in 28 cases with different pathologies and surgeries type was performed with the aim of gaining a better understanding of the nature and extent of the brain shift and the resultant loss of spatial accuracy in surgical procedures co-registered to preoperative imaging studies. Three-dimensional tracking of the cortical surface have been used to quantify the observed motion of a total of 87 cortical points. (Figure 2.8). Data acquisition was facilitated by a ceiling-mounted robotic platform (SurgiScope microscope, ISIS, Saint Martin d'Hères, France) that provided tracking capabilities by focusing the microscope on the same cortical features at the beginning and at the end of surgery. The robotic microscope can memorize its position and thus it is possible to compute the shift of the focused points. Error analysis demonstrated that the surface displacement measuring methodology was accurate to 1-2 mm. Statistical tests were performed to examine correlations between the amount of displacement and the type of surgery, the nature of the cranial opening, the region of the brain involved, the duration of surgery, the degree of invasiveness, and the use of osmotic agents or intentional

CSF drainage. The results show that a displacement of 1 cm on average occurred with the dominant directional component being associated with gravity. Mean displacement was found to be independent of the size and orientation of cranial opening, but to be greater in resective procedures.

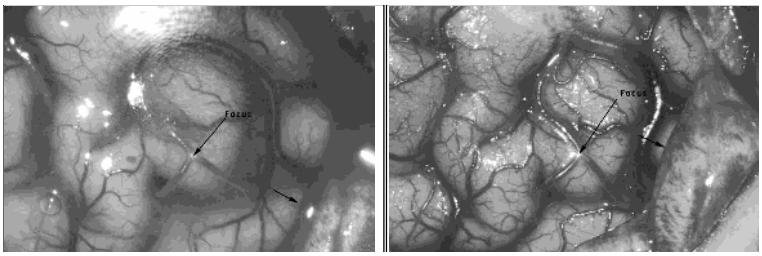

Figure 2.8: 3D displacement. Left Picture was taken shortly after dura mater opening with the focus on a vessel junction (arrow) located at coordinates (232.3, 89.9, 157.5 (mm)). Right picture, acquired 94 minutes later, was taken focusing on the same feature. The feature appears in the same place with respect to the frame but it has moved within the operating field (the arrows in the picture show the dural edge). The coordinates of the focal point are now (234.5, 95.5, 174.3 (mm)) which gives an absolute displacement for that feature of 17.8 mm.

From the result of the previous study the same authors develop a finite element model-based strategy [18]. A 3-D computational model was developed for estimating volumetric displacements and to update the neuronavigational image set (Figure 2.9). The inputs to the model are an estimate of the CSF level for the patient and the patient head orientation for gravity direction estimation. Tissue mechanical properties were based on previous pig brain experiments [19]. Using model calculations, the preoperative image database can be deformed to generate a more accurate representation of the surgical focus during an operation. A preliminary study of four patients that experienced substantial brain deformation from gravity was performed. Cortical shift measurements, performed with the setup above described have been correlated with model predictions. Table 2.1 shows the result of the study comparing the model predicted with the real measured shift. Results over the four cases show that the brain shifted, on average, 5.7 mm in the direction of gravity and that model predictions could reduce this misregistration error to an average of 1.2 mm.

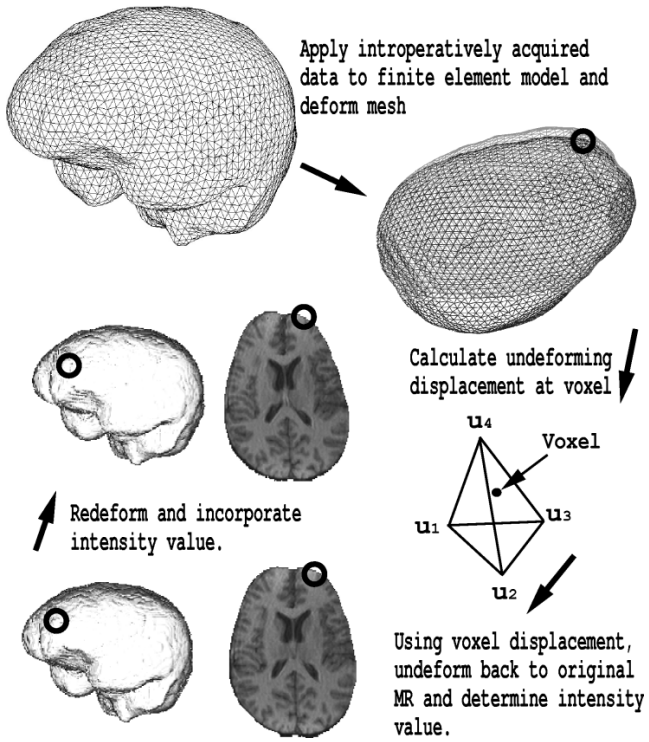

Figure 2.9: Intraoperative image updating algorithm based on model calculated

Subject	Point#	Measured Displ. (mm)	Calculated Displ.(mm)
1	1	6.7	4.9
	2	4.6	5.4
	3	4.2	5.8
	4	3.5	3.4
2	1	10.4	5.7
	2	6.2	6.3
	3	5.9	6.2
3	1	6.1	5.2
	2	5.0	6.5
	3	7.5	6.1
4	1	4.4	4.8
	2	3.5	3.8

Table 2.1: Comparison between measured and calculated shift with respect to gravity

IntraOperative MRI (IMRI) could represents another means of addressing

the changing position of a lesion, as well as key normal structures throughout the course of an operation [28]: obtaining iterative intraoperative MRI, the surgical plan can be altered to account for shift in the position of critical cerebral structures as well as the lesion itself [10]. IMRI is an accurate solution to the brain shift problem but has its drawbacks: the cost benefits rate is not so high and its usages would increase significantly the operative time.

Chapter 3

Materials & Methods

In this chapter a detailed description about the materials, software and the system integration will be given. First of all the commercial navigation system and the software environment (3D Slicer) integrated with this work are described, then the different imaging modality exams available for the clinical study and for intraoperative navigation with the new system will be delineated. In the second part the methods used for the system integration will be outlined together with its added functionalities. In the last part the experimental protocol followed for the clinical study will be given.

3.1 Navigation Hardware

The neuronavigator available at "Claudio Munari" center for Epilepsy Neurosurgey, at "Niguarda Cà Granda" Hospital in Milan is a Medtronic StealthStation TREON Plus. StealthStation TREON is the first infrared system that received the FDA approval. The system allows the bi-dimensional and three-dimensional reconstruction of an anatomic model through the data coming from different imaging modalities such as CT images, MRI, positron emission tomography (PET) and Single Photon emission computed tomography (SPECT).

The system is based on the detection, from a camera, of the infrared light cast back by markers on surgical tools such as the probe, the bipolar or monopolar electrostimulator, or any kind of surgical tool.

3.1.1 System Description

The system is composed by two parts:

1) the navigation system (Figure 3.1) composed by the following parts:

- 18" touchscreen;
- Workstation Silicon Graphics O2;
- DICOM network interface;

- Uninterruptible power supply (UPS);
- CD drive for exams import/export;
- Multi-medial system (Video/audio IN/OUT);
- Foot switch for intraoperative control.

The workstation is particularly stable because the operative system (OS) (IRIX 6.5, a Unix based OS) is suitable for "Critical mission" applications such as surgical procedures. There are audio and video inputs that allows endoscopy or microscope visualization in the same screen. There is a network card that is used for exams transmission in a fast and reliable way. In this case the network interface will also be used to transmit data for the navigation in 3D Slicer.

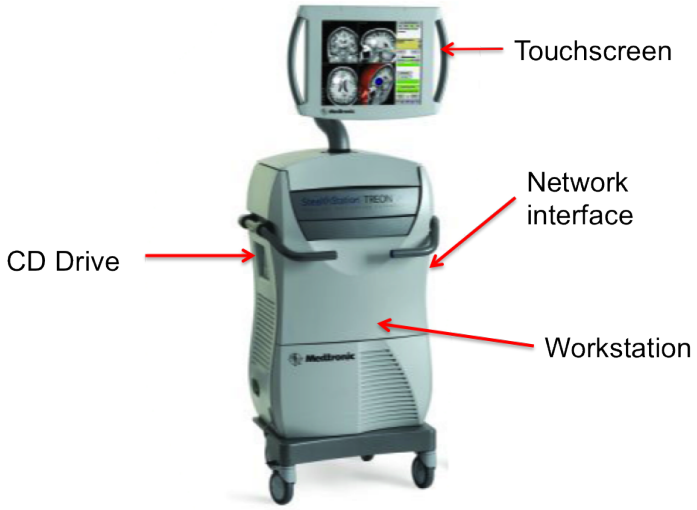

Figure 3.1: The navigational part of the StealthStation® neuronavigation system available at Niguarda Hospital, Milano.

2) An optical system (Figure 3.2) composed by:

- Infrared Polaris Spectra® camera system composed by 3 Charge-Coupled Device (CCD) a laser pointer and an handle. Its accuracy is 0.3 mm and support a maximum update rate rate of 60 Hz (`http://www.ndigital.com/medical/polarisfamily-techspecs.php`). The camera is an hybrid type that can localize both active and passive markers tools;
- Digitalizer that converts data from the camera for the workstation elaboration;

- "Hot plugging" system for tension peak monitoring;

Figure 3.2: The optical system of the StealthStation®.

The two blocks mounted on wheels are independent, allowing the system positioning also in reduced spaces.

3.1.2 Software

There are 4 softwares available on the StealthStation® but one the used in clinical practice at Niguarda Hospital is Mach 5 Cranial version 5.1. This software is specifically dedicated to neurosurgical cranial interventions. Its main features are:

- workflow management following the user from the preoperative phase, to the planning, setup and navigation phases (paragraph 3.1.3);
- automatic tool recognition in order to activate the closest tool to the operative field without the need to manually select the tool that the system must track;

- fast skin 3D model reconstruction (ray casting from the threshold segmented volume);
- images fusion software integrated. The system allows to load 2 ore more exams of the same patient and merges them automatically through a registration procedure;

3.1.3 Surgical procedure workflow

The navigator is useful in different phases of the operation and the software follows the set-up in all the operative phases.

- In the preoperative phase the surgeon load one or more exams on the system. If the exams are more than one they are automatically coregistered. The skin 3D model is then computed.
- The intraoperative phase is composed by four steps (Figure3.3):
  1. patient's head fixing with the Mayfield head frame (left picture);
  2. optical system tracker positioning;
  3. reference frame connection to the Mayfield clamp (right picture);
  4. registration (paragraph 3.1.4).

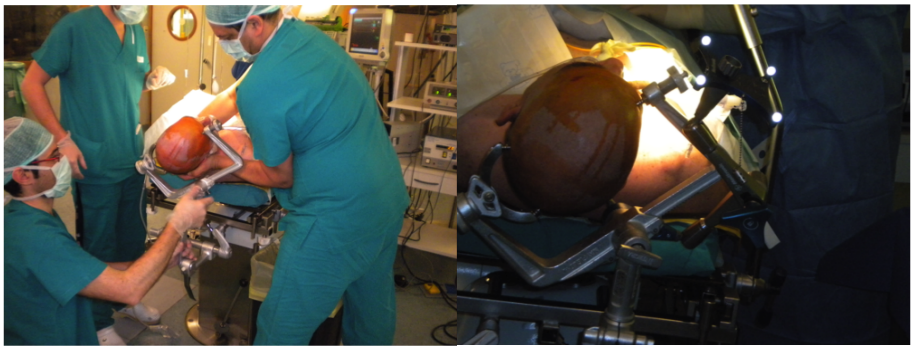

Figure 3.3: The main phases of the patient set-up for allowing navigation in a neurosurgery operation. Left: the Mayfield head frame positioning to the patient head; Right: the reference frame attached to the Mayfield clamp.

Those procedures are made in a non sterile field. After registration has been performed the surgery could start in a sterile field (the probe and the reference frame are then substituted by sterile ones, Figure 3.4).

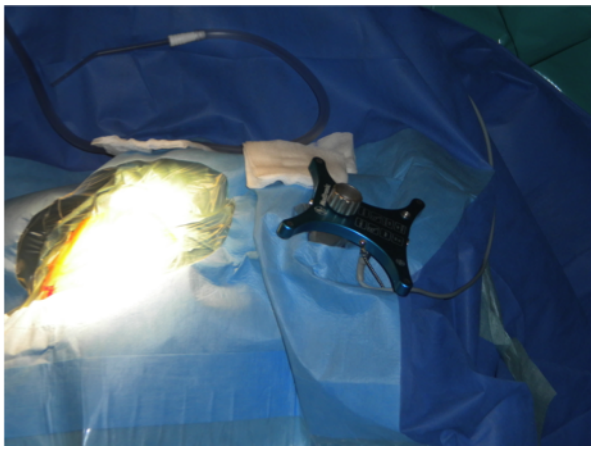

Figure 3.4: Sterile field. It is recognizable the reference frame close to the patient head covered by sterile paper.

The last phase is the navigation phase: whenever the foot-switch is pressed the surgeon can see the three 2D orthogonal views centered on the navigated point (i.e currently tracked tool tip - Figure 3.5 right).

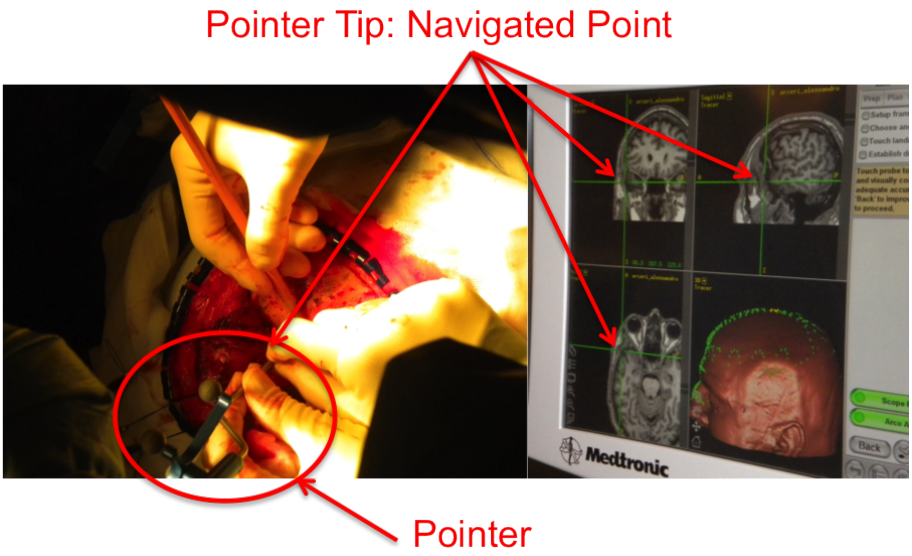

Figure 3.5: Target recognition helped by neuronavigator. The Probe is in the surgeon hand, that press the foot switch and then check the navigator screen (at the right). At this point trace a pencil sign on the bone.

3.1.4 Registration methods supported

The registration is the core phase of a navigation procedure. The StealthStation software provides two different ways to register a patient a point to point registration (PointMerge®) and a surface registration method(Tracer®).

PointMerge® PointMerge® is a typical point to point registration procedure [32] that relies on the matching between correspondent point in two different coordinates system. The step of this procedure are (Figure 3.6):

1. selecting with the mouse from 4 to 10 anatomical points on the exam 3D model (bottom right of the screen);
2. touching with the pointer one of the correspondent anatomical points on the patient;
3. pressing the foot switch for storing each touched point;
4. repeating step 2-3 for all the points selected in 1;
5. checking the estimated registration accuracy provided by the software.

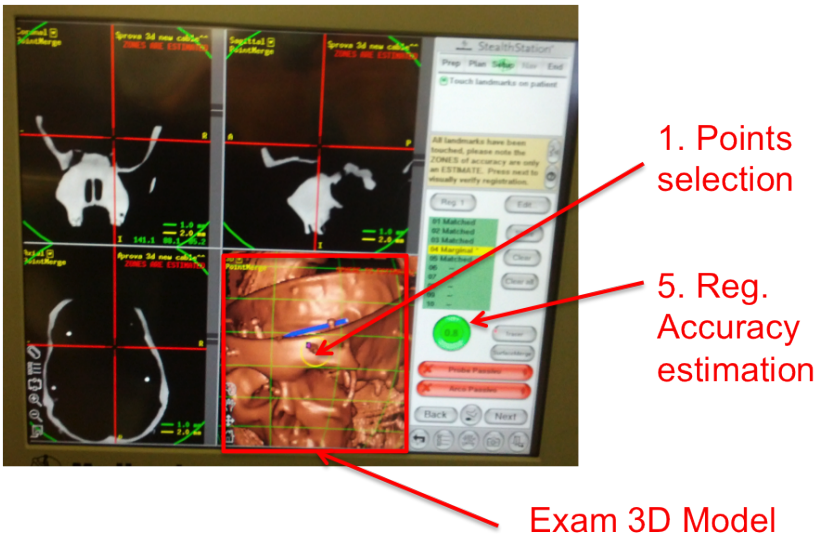

Figure 3.6: Point to point registration procedure used for the phantom accuracy study.

Tracer® Tracer® is the registration method used in the clinical routine at Niguarda Hospital. It is a particular implementation of a surface registration method [2]. The procedure requires the following steps:

1. touching with the pointer the nose tip and pressing the foot-switch;
2. touching with the pointer point in the middle of the front and pressing the foot-switch;
3. touching with the pointer a point at about 3 cm at the left of the point touched in step 2 and pressing the foot-switch;
4. acquiring at least 256 point covering the whole skin surface keeping pressed the foot-switch (Figure 3.7). It is clinical practice to acquire at least 600 points.

The software fits the acquired point on the 3D model surface computing the registration matrix as result. This registration modality does not give as output the estimated registration accuracy

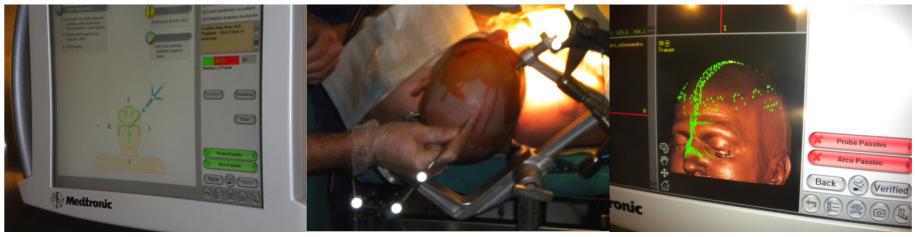

Figure 3.7: Two phases of the Surface registration workflow. The picture at the left suggests the regions to acquire, the one at the centre shows the point collecting phase and the one at the right represent the points collected.

3.2 3D Slicer 4

3D Slicer [9] is a free open-source software application for medical images visualization and computing developed by the Surgical Planning Laboratory of Brigham & Women's Hospital (Boston, Massachusetts USA), Kitware inc. (Clifton Park, NY) and the Slicer community. As a clinical research tool, 3D Slicer is similar to a radiology workstation that supports versatile visualizations (Figure 3.8) but also provides advanced functionality such as automated segmentation and registration for a variety of application domains. Unlike a typical radiology workstation, 3D Slicer is free and is not tied to specific hardware. As a programming platform, 3D Slicer facilitates translation and evaluation of the new quantitative methods by allowing the biomedical researcher to focus on the implementation of the algorithm and providing abstractions for the common tasks of data communication, visualization and user interface development. Compared to other tools that provide aspects of this functionality, 3D Slicer is fully open source and can be readily extended and redistributed. In addition, 3D Slicer is designed to facilitate the development of new functionality in the form of 3D Slicer extensions.

Its extendible platform makes use of different toolkits for various purposes: for visualization and 3D graphics algorithms it uses the Visualization Toolkit (VTK) (`http://www.vtk.org/`), for the graphical user interface (GUI) it uses Qt (`http://qt-project.org/`) and CTK (`http://www.commontk.org/` specifically designed for biomedical applications), ITK (`http://www.itk.org/`) is used for medical specific algorithm such as image registration, segmentation and image filtering, for datasets import nrdd package (`http://teem.sourceforge.net/nrrd/`) is used.

Its main features include:

- Available for windows, linux and Mac OS X;
- Support for many modalities, including, MRI, CT, US, DTI, nuclear medicine, and microscopy;
- Robust support for DICOM;
- Flexible display capabilities with a variety of predefined layouts for slice reformats and 3d views;
- Annotations;
- Accelerated volume rendering;
- Powerful data fusion and registration capabilities;
- Automated and interactive segmentation tools Surface reconstruction from image data (Marching Cubes, Isosurface modelling);
- Bidirectional interface for devices (OpenIGTLink);
- Plugin architecture for IO formats and algorithms Extensible & scriptable development platform (C++/Python).

Slicer is capable to load 3D surface models such as FreeSurfer (`http://ftp.nmr.mgh.harvard.edu/`) pial and white matter models of the brain, obtained though state of the art segmentation technique. Those models are particularly realistic reconstruction of cortical structures computed with segmentation methods specifically developed for brain MRI [5]. This Slicer capabilities is one of the reason that lead the integration of the Medtronic navigator in this environment.

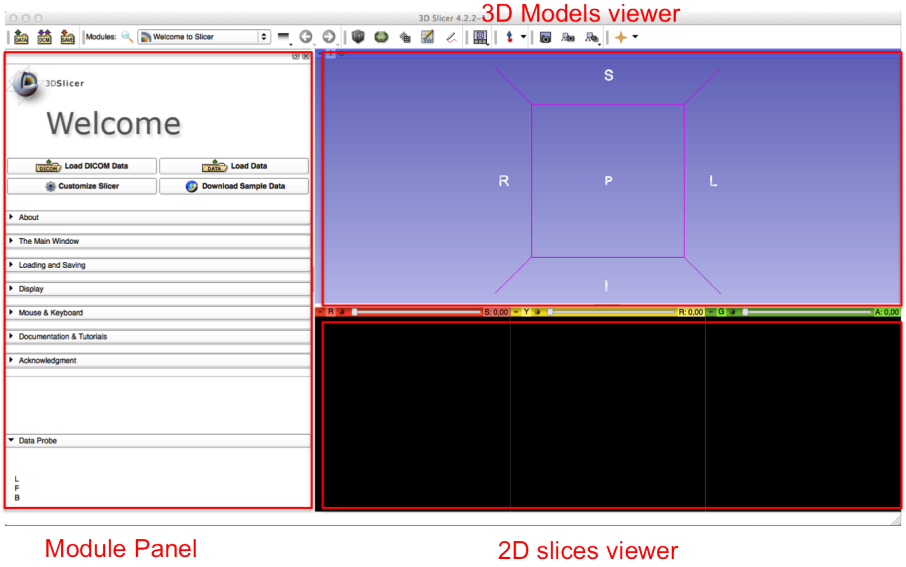

Figure 3.8: 3D Slicer default interface. At the left panel different modules enable the system to be extremely flexible and modular, in the upper part there is the 3D Models viewer, and at the bottom it possible to visualize the 2D slices views of volume loaded and currently selected.

3.3 Input Data

Epileptic patients undergoing surgical resection at Claudio Munari center (Niguarda Hospital) performed the following examinations:

1. 3-dimensional (3D) MRI T1-weighted of the brain (scanned with Intera Achieva, Philips Medical System, The Netherlands), acquired on the sagittal plane and reformatted into axial slices with 560 x 560 matrix, 0.46 x 0.46 x 0.9 mm voxel, and no inter slice gap;

2. 3D rotational angiography acquired in frameless and markerless conditions outside the operating room with O-arm 1000 System (Medtronic, Minneapolis, Minnesota), a mobile cone-beam CT scanner that ensures 0.4 x 0.4 x 0.8 mm reconstructed voxels, to obtain 3-D digital subtraction angiography (DSA);

In some cases Fluid attenuated inversion Recovery (FLAIR) MRI, fMRI, Diffusion Tensor Imaging (DTI) and Computed Tomography (CT) scans where also available.

3.3.1 Data processing

Data are processed with the following workflow:

1. The MRI is registered to the angiography (reference space) using an open-source software (FSL - `http://fsl.fmrib.ox.ac.uk/fsl/fslwiki/`);
2. The cortical ribbon is extracted from the registered MRI using FreeSurfer cortical segmentation methods[5];
3. pial and white matter 3D surface are computed by FreeSurfer;
4. Scalar fields are computed and overlayed to the pial model: thickness of the cortex for each point and sulcality value (i.e an index of the proximity to sulcus);
5. The subcortical volume is again segmented using atlases;
6. All the processing output are loaded in 3D Slicer.

In figure 3.9 it is shown the processing workflow.

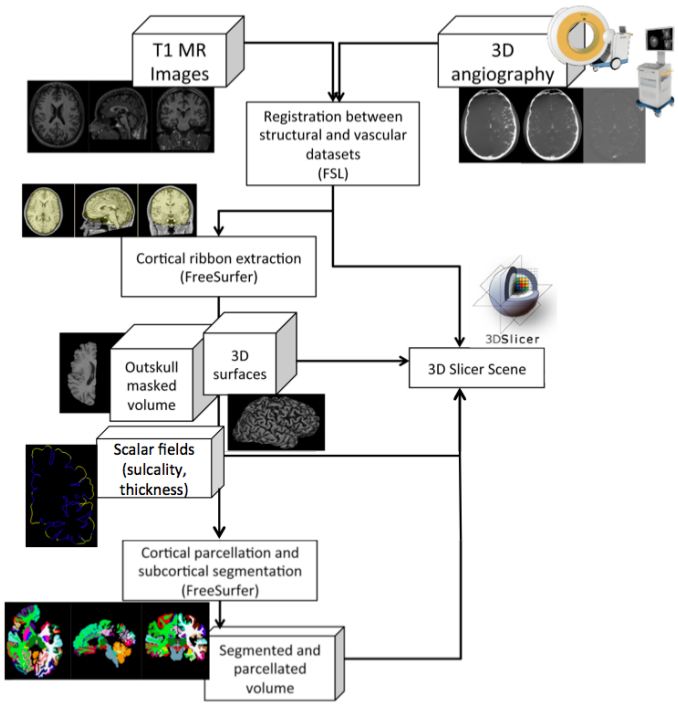

Figure 3.9: Imaging processing workflow starting from the input data to the final 3DSlicer scene.

A typical 3D Slicer scene used for navigation is represented in Figure 3.10.

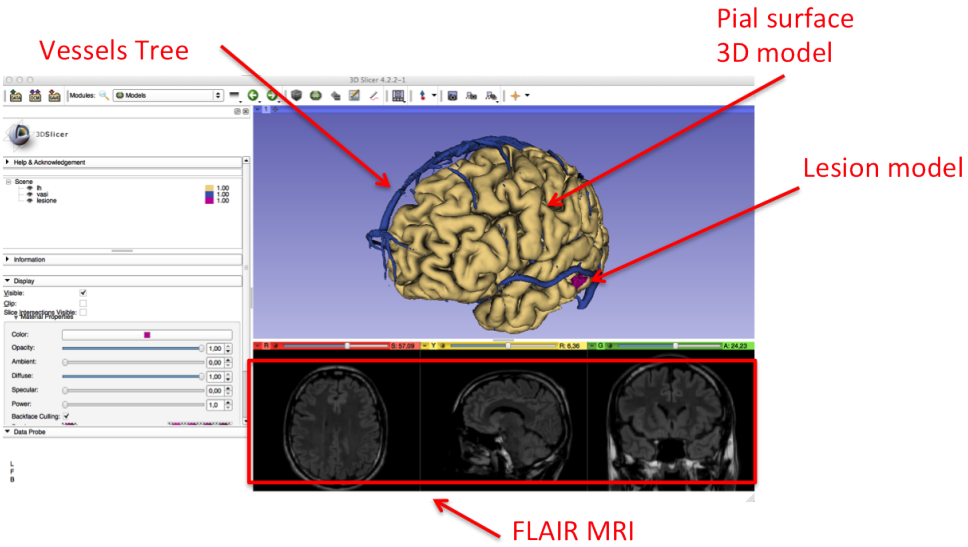

Figure 3.10: A typical 3D Slicer scene: it is visible the pial surface 3D model, the vessels tree, a model of the lesion and the 2D views of the FLAIR MRI..

3.4 Communication protocols

StealthLink is used to access data from Stealthstation, while OpenIGTLink is used for communication with 3D Slicer.

3.4.1 Stealthlink

StealthLink is the application program interface (API) provided by Medtronic (`http://www.na-mic.org/Wiki/index.php/Stealthlink_Protocol`) for research purposes. We obtained the version 1 through a license agreement signed between Politecnico di Milano and Medtronic. The API is a simple query/retrieve interface with static data structures, available for the software applications (paragraph 3.1.2) on the StealthStation and running under Windows and Linux. Client / Server [1] communication is established through sockets. Usually multiple client programs can share the services of a common server program, but the StealthLink server installed on the StealthStation only allows a maximum of 5 connections per session.

The StealthLink version obtained for this thesis work is the Windows one. In particular we obtained from Medtronic:

1. the API header files (.h);

[1] an architecture that describes the relationship between two computer programs in which one program, the client, makes a service request to another program, the server, which fulfills the request.

2. the compiled static library files (.lib) compiled and only compatible with Microsoft Visual Studio 2005;

3. a Demo version of the client with the possibility to print out the current location transforms of the tracked tool, of the reference frame and the registration transform.

Data available via StealthLink 1 include:

- calibration transforms for multiple tools;
- reference frame transformations;
- image space to frame space registration transforms;
- Registration information (type, accuracy);

All transforms are represented by 4x4 matrixes and points coordinates by 3x1 vectors.

3.4.1.1 Application Program Interface

The API provides the following functionalities[30]:

Tracked Tool Information The GET_TOOL function provides information on the selected tool. It returns the tool name, tool position and orientation, and tool geometry error of the tool currently being tracked by the StealthStation® system. Tool geometry error reveals errors in the LED or sphere configuration on the instrument. If the tool geometry error exceeds 0.5 millimeter, the device may be significantly bent or otherwise damaged. If the selected tool is not visible to the localizer, no information is returned and the value of the valid flag is "False".

Reference Frame Information The GET_FRAME function provides information on the patient reference frame. It returns the patient Reference name, position, orientation, and geometry error. If the patient reference is not visible to the localizer, no information is returned and the value of the valid flag is "False".

Registration Information The GET_REGISTRATION function provides information on the registration performed. It returns the transform for the reference frame to image coordinates and the predicted accuracy. The predicted accuracy value is the predicted maximum localization error you may encounter anywhere on the surface of an imaginary sphere 10cm in radius centered at the centroid of the selected landmarks. Because localization error generally decreases as you move closer to the geometric midpoint of the selected landmarks, this value can be thought of as an upper limit on the error you would encounter

while navigating anywhere within this imaginary sphere. The predicted accuracy value is only valid for point-based registration such as PointMerge®. If the patient registration has not been performed, the value of the valid flag is "False".

Exam Information The GET_EXAM_INFO function returns information about the loaded patient exam. This includes the voxel dimension and the patient volume size in voxels.

3.4.2 OpenIGTLink

OpenIGTLink an open network protocol for image-guided therapy (IGT) specifically developed for operating room devices communication [31].

The protocol is able to transfer positional data with sub-millisecond latency up to 1024 fps and images with latency of less than 10 ms at 32 fps. The protocol not only improves the interoperability of devices and software, but also promotes transitions of research prototypes to clinical applications (section 2.2, [22]). In fact with the increasing number of IGT applications and the availability of Ethernet in the IGT environment, standardization of information and communication technology is more important than ever.

For the implementation of an OpenIGTLink compliant software the developer can choose between three approaches:

- implementing from zero OpenIGTLink functionalities following the protocol, this is useful only when there is the necessity to write the software in a language different from C/C++;
- using simple C code (igtlutil). This code provides C structures for the generic header, image header and transform header, and supporting functions to create a message packet. It is suitable for applications written in C and C++ and is implemented just by copying the source files into the source directory. A socket implementation is not provided thus the developer needs to use an external socket implementation;
- using the Open IGTLink Library. The library supports C++ classes to create OpenIGTLink messages. TCP/IP communication via socket is already implemented. This is the most convenient and safe way for an OpenIGTLink compliant implementation.

OpenIGTLink is the standard embedded communication protocol in 3D Slicer. A special module in the software allows sending and receiving data from the Slicer scene to external devices that support the protocol.

3.5 System integration

In this section the system integration between the Medtronic navigator and the 3D Slicer environment will be described.

The integrated system is composed by three blocks: the StealthStation®, a Windows client running on a Virtual Machine (VM), developed in order to retrieve data from the navigator, and a self developed navigator module running into 3DSlicer on Mac, that receives data from the Windows client and uses them for navigation. StealthStation and Mac are connected to the hospital network through ethernet interface.The network protocol used for the communication between blocks are visible in Figure 3.11.

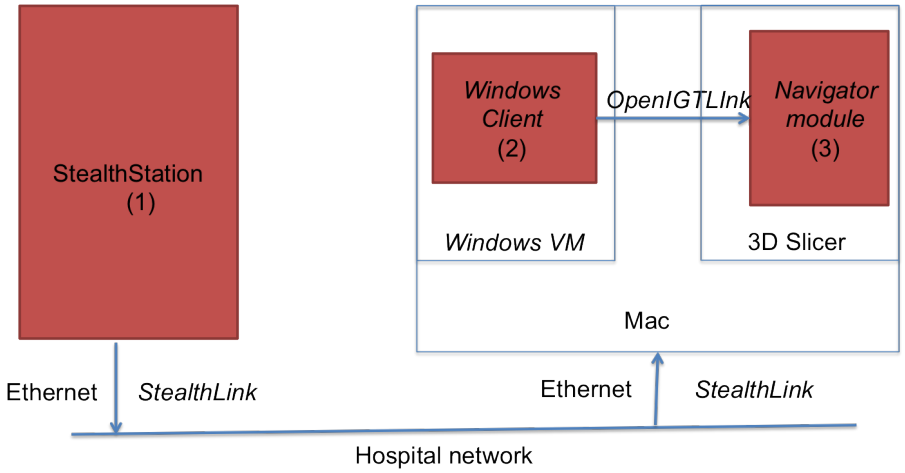

Figure 3.11: The StealthStation® is connected via Ethernet interface to the Mac: the protocol used is StealthLink. On the Mac a Windows Virtual Machine (VM) is running and a Windows Client retrieve data from the StealthStation. The Windows client process and send data to 3D Slicer using the OpenIGTLink protocol.

StealthStation was already described in section 3.1. In the following paragraph the other two system components are described in detail.

3.5.1 Windows Client

The Windows client allows the communication between the StealthStation® and 3D Slicer (Figure 3.12). It is written in C/C++ and compiled with the StealthLink libraries with Microsoft Visual Studio 2005. The Integrated Development Environment (IDE) used is Visual Studio 2005. The software is composed by four blocks dedicated to:

1. connecting to the StealthStation® and 3D Slicer;
2. data retrieving from the StealthStation®;
3. computation of the necessary geometric transformation;

4. sending the output transforms to 3DSlicer (navigator module, described in paragraph 3.5.2).

Blocks 2-3-4 of the software are embedded in a loop that every 100 ms retrieve data, process them and continuously send transforms to Slicer.

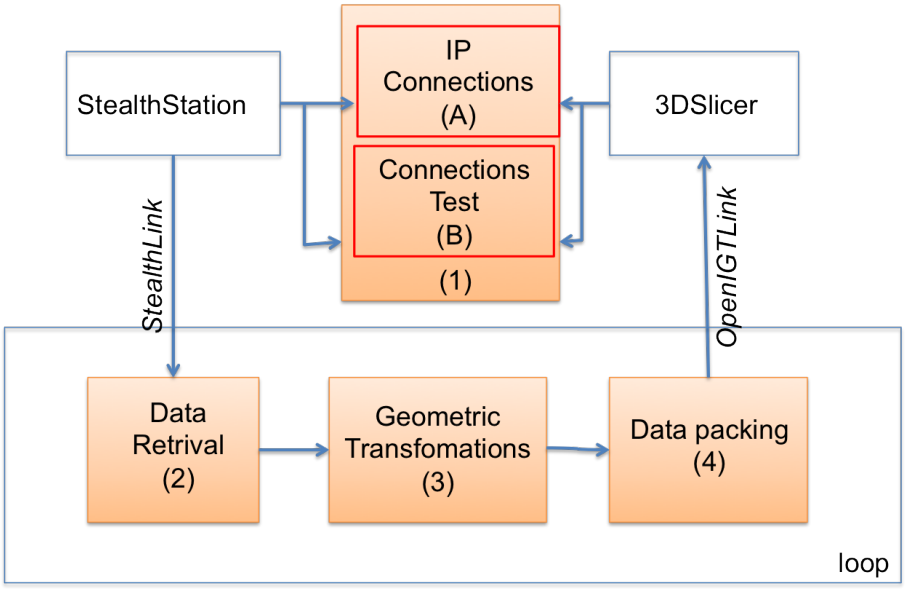

Figure 3.12: Block diagram of the Windows Client.

Block 1 (Figure 3.12) is divided in two logical parts:

A- connection of the client to the StealthStation® software and to 3D Slicer. The client connection is enabled by the user that must set the StealthStation® and the Mac internet protocol (IP) address.

B- data retrieval and printing for testing both the communications of A.

Block 2 (Figure 3.12) is dedicated to data retrieval from StealthStation. The data obtained by the client through StealthLink are:

- the patient exams size;
- the registration transform;
- the reference frame transform (i.e patient transform);
- the pointer (currently tracked tool) transform;
- the calibration of the tool tip.

Block 3 transforms the raw data received into a common reference system: the 3D Slicer image space (Figure 3.13). [2] For matrix computations an external C++ library (`http://www.techsoftpl.com/matrix/`) was used.

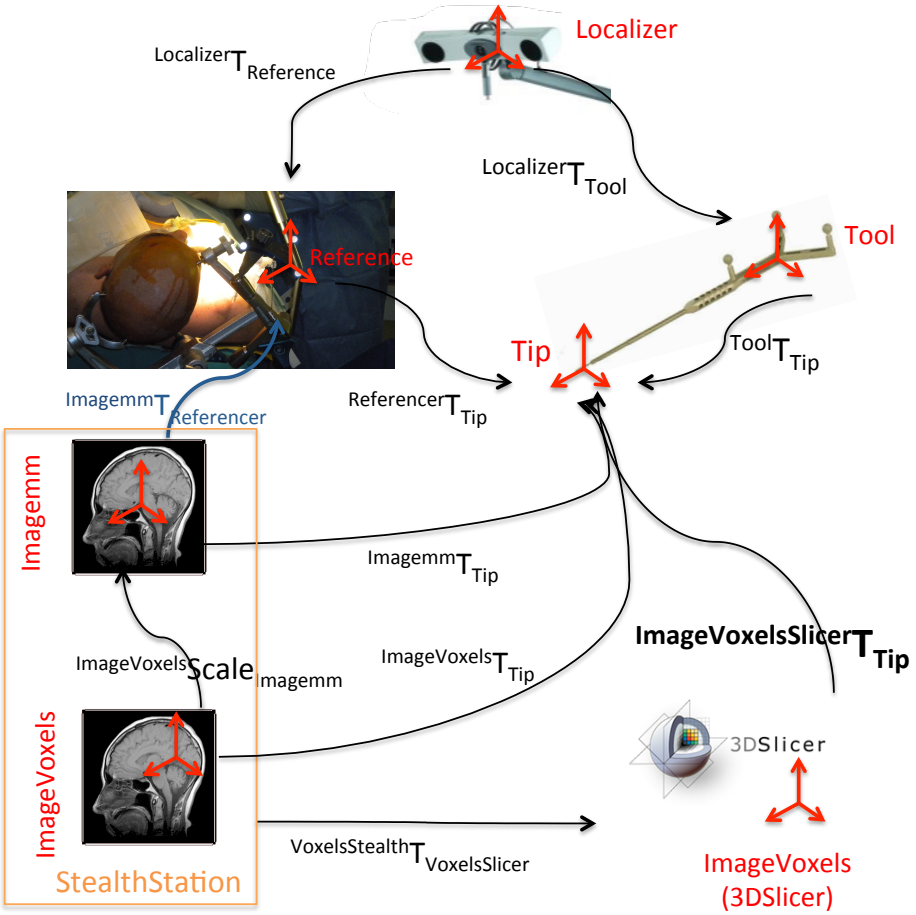

Figure 3.13: Geometric transformations performed by the Windows client.

The performed transformations are represented in the following equations. where **T** represents (4x4) matrix transforms and P (3x1) represents coordinates vectors.

The pointer tip is reported in the localizer reference system through the tip calibration transformation, ${}^{\mathbf{Tool}}\mathbf{T}_{\mathbf{Tip}}$ by equation 3.1

$$ {}^{\mathbf{Localizer}}\mathbf{T}_{\mathbf{Tip}} = {}^{\mathbf{Localizer}}\mathbf{T}_{\mathbf{Tool}} \cdot {}^{\mathbf{Tool}}\mathbf{T}_{\mathbf{Tip}} \tag{3.1} $$

[2] The geometric transforms are computed using homogeneous transforms in the form of 4x4 matrix. Raw data are C matrix (float[4][4]).

Where: ${}^{\mathbf{Localizer}}\mathbf{T}_{\mathbf{Tool}}$ is the tool to localizer 3D transformation and

$${}^{\mathbf{Tool}}\mathbf{T}_{\mathbf{Tip}} = \begin{bmatrix} 1 & 0 & 0 & {}^{Probe}P_{Tip}(1) \\ 0 & 1 & 0 & {}^{Probe}P_{Tip}(2) \\ 0 & 0 & 1 & {}^{Probe}P_{Tip}(3) \\ 0 & 0 & 0 & 1 \end{bmatrix}$$

where ${}^{Tool}P_{Tip}$ is the calibration vector of the tool provided by the StealthStation. The calibration transformation was used instead of the calibration vector in order to obtain also the tool orientation in image space.

Next, the tool tip coordinates are reported in the reference frame space (eq. 3.2). This is done in order to obtain the independence of the tracking from the relative movements localizer - patient

$${}^{\mathbf{Reference}}\mathbf{T}_{\mathbf{Tip}} = ({}^{\mathbf{Localizer}}\mathbf{T}_{\mathbf{Reference}})^{-1}.{}^{\mathbf{Localizer}}\mathbf{T}_{\mathbf{Tip}} \tag{3.2}$$

$({}^{\mathbf{Localizer}}\mathbf{T}_{\mathbf{Reference}})^{-1}$ is the inverse of the reference frame to localizer 3D transformation.

Then, the tool coordinates in image space (in millimeters) is obtained:

$${}^{\mathbf{Imagemm}}\mathbf{T}_{\mathbf{Tip}} = {}^{\mathbf{Imagemm}}\mathbf{T}_{\mathbf{Reference}}.{}^{\mathbf{Reference}}\mathbf{T}_{\mathbf{Tip}} \tag{3.3}$$

${}^{\mathbf{Imagemm}}\mathbf{T}_{\mathbf{Reference}}$ is the registration transform from the StealthStation image space (millimeters) to the reference frame space. The registration procedure is completely demanded to the StealthStation® and the method used in our set-up is the Tracer® surface registration.

One of the last transform computed is the conversion of the coordinates from millimeters to voxels.

$${}^{\mathbf{Imagevoxels}}\mathbf{T}_{\mathbf{Tip}} = {}^{\mathbf{Imagevoxels}}\mathbf{Scale}_{\mathbf{Imagemm}}.{}^{\mathrm{Imagemm}}\mathrm{T}_{\mathrm{Tip}} \tag{3.4}$$

with

$${}^{\mathbf{Imagevoxels}}\mathbf{Scale}_{\mathbf{Imagemm}} = \begin{bmatrix} 1/Sag_{sp} & 0 & 0 & 0 \\ 0 & 1/Cor_{sp} & 0 & 0 \\ 0 & 0 & 1/Ax_{sp} & 0 \\ 0 & 0 & 0 & 1 \end{bmatrix}$$

where $Sag_{sp}, Cor_{sp}, Ax_{sp}$ are the Sagittal, Coronal and Axial voxels spacing of image loaded in StealthStation®. At this point the 3D coordinates of the voxels in image space of the exam loaded in the StealthStation are obtained.

The last transformation performed by the Windows client is necessary for the conversion from the StealthStation® image reference system to the Slicer one. A clockwise 180° rotation around the StealthStation image Sagittal axis and a translation along the Coronal and Axial axes are performed. The translations are equal to the exam size in each dimension (axial and coronal).

The resulting transformation has the following form:

$$^{\mathbf{VoxelsStealth}}\mathbf{T}_{\mathbf{VoxelsSlicer}} = \begin{bmatrix} 1 & 0 & 0 & 0 \\ 0 & -1 & 0 & Size(Cor) \\ 0 & 0 & -1 & Size(Ax) \\ 0 & 0 & 0 & 1 \end{bmatrix}$$

Where $Size(Cor)$ and Size(Ax) are respectively Coronal and axial dimensions of the exam loaded in the StealthStation.

$$^{\mathbf{ImageVoxelsSlicer}}\mathbf{T}_{\mathbf{Tip}} = ^{\mathbf{VoxelsStealth}}\mathbf{T}_{\mathbf{VoxelsSlicer}} \cdot ^{\mathbf{Imagevoxels}}\mathbf{T}_{\mathbf{Tip}} \quad (3.5)$$

Where $^{\mathbf{ImageVoxelsSlicer}}\mathbf{T}_{\mathbf{Tip}}$ represent the voxels coordinates of tool tip and the tool orientation in the Slicer reference system.

As said **Block 4** (Figure 3.12) of the Windows client sends the $^{\mathbf{ImageVoxelsSlicer}}\mathbf{T}_{\mathbf{Tip}}$ transform to the 3D Slicer navigator module (paragraph 3.5.2) using OpenIGTLink protocol. Once the bit stream is generated, the package is sent to Slicer, through the network, using a socket. For this purpose, the standard windows socket library was used.

The main feature of this client is that it is able to manage two different connections with opposite direction and to different servers (StealthStation® and Slicer).

Windows Client set-up In order to start the navigation few steps must be followed on the Windows client. A screenshot of the user interface is shown in Figure 3.14:

1. Setting StealthStation IP address
2. Connect the client to the StealthStation
3. Set the Mac IP address
4. Press the start button.

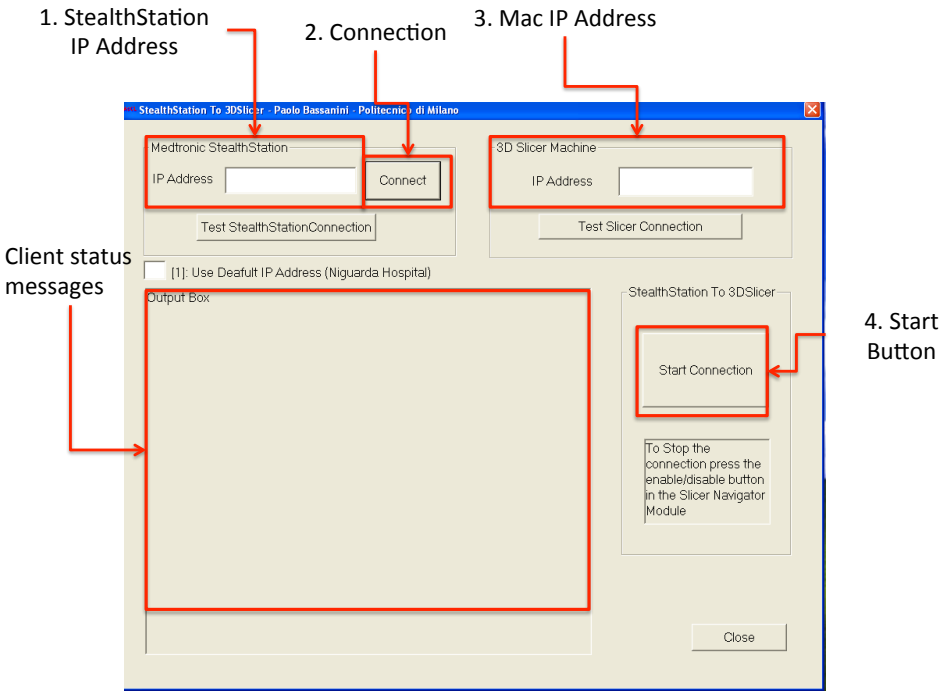

Figure 3.14: A screenshot of the Windows client. In the upper part the IP address of the StealthStation and of the Slicer workstation has to be set (Point 1 and 3 in figure), two buttons are dedicated to communication testing. In the central part a message window will show messages about the client status, at the right the main START button (point 4), that enable all the infinite loop of blocks 2, 3 and 4 continuously sending transforms to 3DSlicer.

3.5.2 Navigator module

In order to navigate in 3D Slicer, a dedicated software application was developed. The main functionalities of the module are:

- setting up the Slicer environment for receiving data from the Windows client;
- transform received data for the specific exam loaded in 3DSlicer;
- giving to the user some extra functionalities.

Slicer Navigator module set-up To usage of the module for navigation requires that the user (Figure 3.15):

1. enables the communication with the Windows client pressing the dedicated button;

2. load in 3D Slicer the exams that will be used for navigation;
3. press the Initialize button;

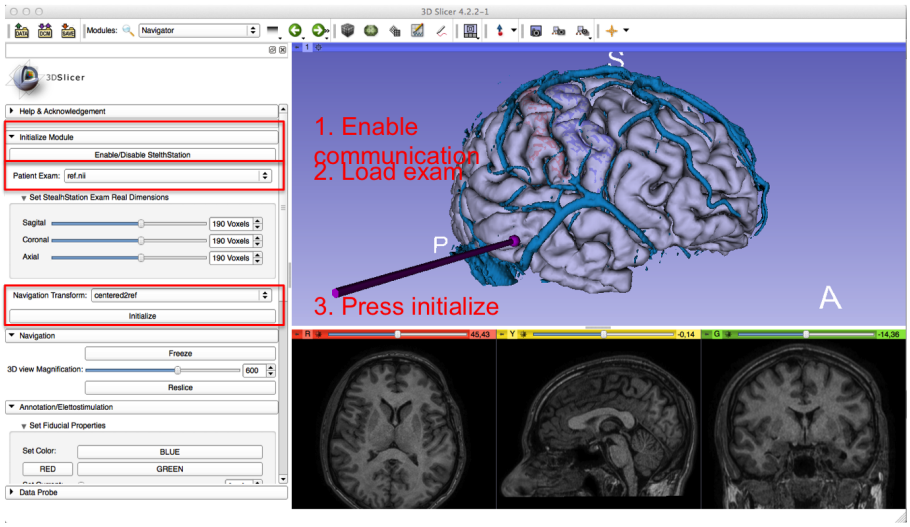

Figure 3.15: 3D Slicer GUI scene with a virtual tool (fuchsia) representing the navigator tool.

The module was developed as a python script, and it results embedded in the Slicer environment (Figure 3.15). This software is dived in 4 blocks:

1. Module initialization (Figure 3.15);
2. Navigation panel (Figure 3.16);
   (a) Freezing functionality;
   (b) Reslice functionality;
3. Annotation panel (Figure 3.18);
4. Two extra functionalities: Virtual Craniotomy and Full trajectories collection.

In the **first block** the OpenIGTLink connection is set up enabling the communication with the Windows Client. The received transform ${}^{\mathbf{ImageVoxelsSlicer}}\mathbf{T}_{\mathbf{Tip}}$ can not be directly used for navigation of the Slicer scene. It must be transformed to the reference frame of the specific exam loaded in 3D Slicer:

$$ {}^{\mathbf{RAS}}\mathbf{T}_{\mathbf{Tip}} = {}^{\mathbf{RAS}}\mathbf{T}_{\mathbf{Voxels}} * {}^{\mathbf{ImageVoxelsSlicer}}\mathbf{T}_{\mathbf{Tip}} $$

The ${}^{\mathbf{RAS}}\mathbf{T}_{\mathbf{Voxels}}$ transform matrix is extracted from the exam header and represents the loaded exams voxels spacing and orientation in the Slicer reference frame. RAS stands for Right Anterior Superior and is the slicer reference frame. ${}^{\mathbf{RAS}}\mathbf{T}_{\mathbf{Tip}}$ is finally used to pilot a virtual tool (a calibrated VTK model) that will be active during navigation (Figure 3.15).

The **second block** is the **Freezing functionality**. During navigation the virtual model of the tracked tool continuously moves. It is very useful instead to freeze the situation at a specific moment. For example if the surgeon wants to understand if a specific point in the brain is close or not to the lesion or tumor he can touch the point, freeze the situation, remove the pointer and then analyze the exams of the 3D scene.

This functionality enables to freeze the scene at the currently tracked coordinates. By pressing the "Freeze" button the orthogonal 2D views of the patient exam are centered in the point tracked by the pointer. Additionally also the 3D scene is reoriented. The view plane of the virtual camera is set orthogonal to the pointer main axis orientation (Figure 3.16). It is also possible to set the zoom of the camera setting the dedicated slider in the user interface.

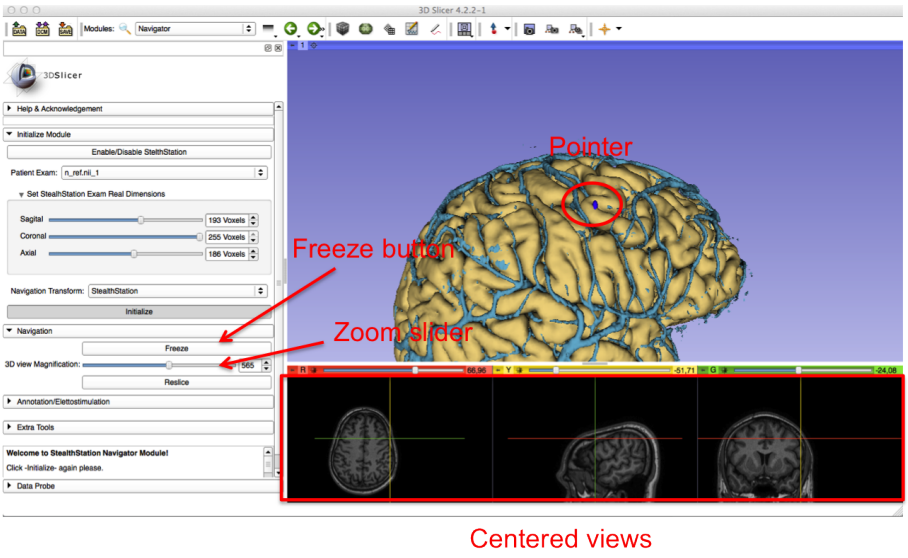

Figure 3.16: Freezing and tool virtual camera. The pointer is not visible (only a blu dot is visible) because the camera view plane is set orthogonal to the main pointer axis.

The **Reslice functionally** is the possibility to reslice the 2D images along the main pointer axis. In that case the surgeon will see the 2D views of the exams centered in the point currently tracked by the navigator, with the 2D views reformatted (Figure 3.17): the normal of slicing plane will be the pointer main axis in the first viewer. The other two viewer will show the volume resliced

along the other 2 orthogonal planes.

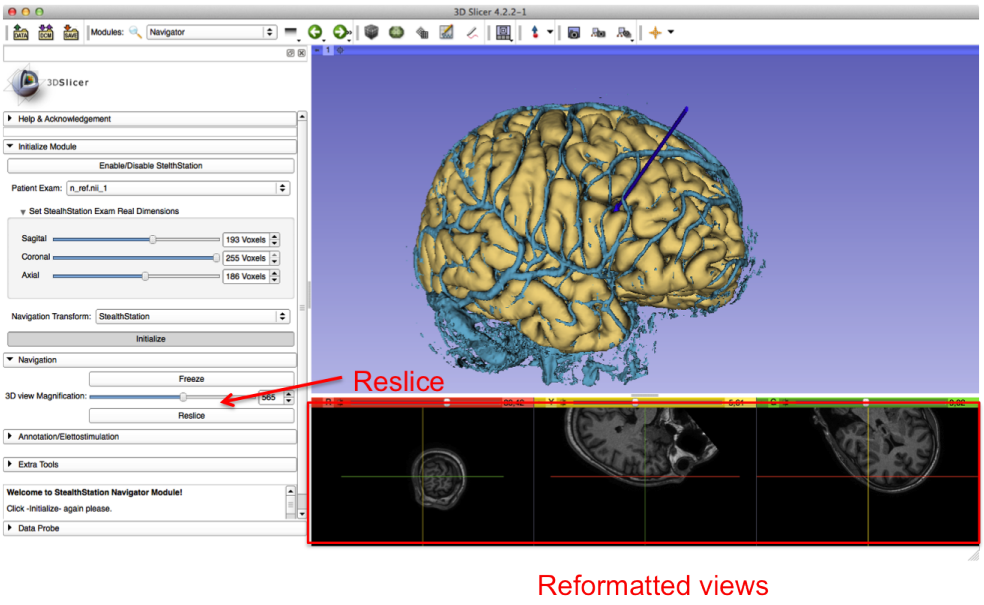

Figure 3.17: Reslicing feature: pressing the button "Reslice" during navigation the exams 2D views are reformatted according to the tool orientation.

The **third block** is the **Intraoperative Annotations** function. The surgeon can add to the 3D scene the localized annotations. The annotations are represented by default 3D Slicer annotations called "Fiducials". In 3D Slicer it is possible to place fiducials selecting a point in the 3D scene with the mouse, there was not the possibility to add fiducials at location defined by a navigated pointer. In particular with the module the fiducials are placed in the point correspondent to the pointer tip.

The feature is used in two clinical situations:

1. DES results annotations and notification: electrical stimulator used for DES can be be tracked in the 3D Slicer scene. During the stimulation the user can store relevant stimulation points. A dedicated panel in the Navigator module provide the following functions:

   (a) get the currently tracked position;

   (b) set a name or description of the specified point (for example the cortical motor area mapped);

   (c) annotate the stimulation current used;

   (d) setting the color of the spherical object that will be generated in the scene at the selected location (Figure 3.18);

(e) storing and visualize the object in scene if the stimulation is considered relevant.

A color code established at Niguarda Hospital has been: RED (to represent an area/region that should be preserved), GREEN (a point that could be removed because the electrostimulation did not mapped the point as an eloquent region). The surgeon will use the fiducials placed as resection limits, and since they will be always visible on the Slicer scene they can be easily monitored.

2. Brain shift monitoring: annotations can be placed on the same fiducial point in different phases of the surgery for monitoring brain displacement. A clinical study has been performed using the feature for this purpose (section 3.7).

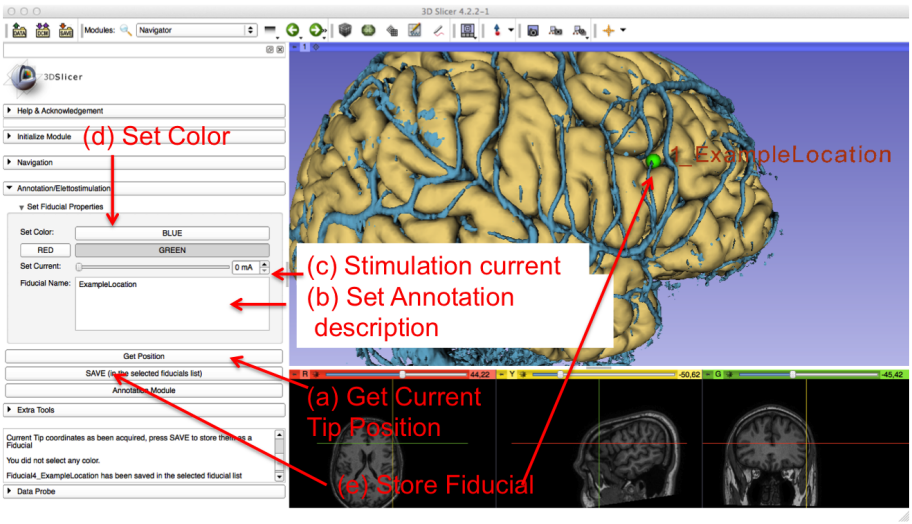

Figure 3.18: Intraoperative annotation feature.

Virtual craniotomy. For the virtual craniotomy computation the module requires that the surgeon acquires some points along the border of the performed craniotomy using the "Intraoperative Annotations" feature.

- the module set those points as the vertices of a polygon;
- The plane approximating the acquired points is computed and the polygon is extruded along the plane normal direction (3 cm up and 3 cm down the skull surface).
- A difference boolean operation provided by the Visualization ToolKit (VTK) is performed between the skull model and the extruded polygon. The VTK class used is

vtkBooleanOperationPolyDataFilter

and the methods are

SetOperationToDifference(), GetOutput()

This result in a hole in the skull model that accurately represents the craniotomy (Figure 3.19).

With the same function it is possible to acquire and represent on the scene the dura mater opening.

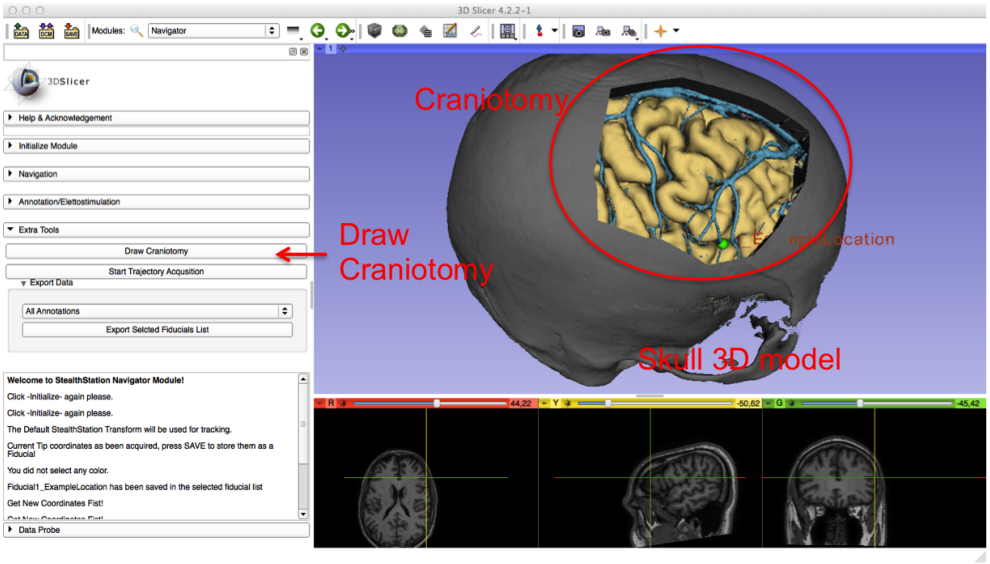

Figure 3.19: Virtual craniotomy feature. It is shown a real scene used during a surgical intervention in which the skull 3D model of the patient (gray) was modified by the Virtual Craniotomy Function. The hole in the skull represents the performed craniotomy.

Full trajectories collection

Its functionality is to export in a text file **all the coordinates** acquired during a surgical gesture with the probe. The output data could then be subjected to further analysis. The tool was used is conjunction with the "Intraoperative annotation" feature to collect data for the following described studies.

3.6 System accuracy evaluation

The overall accuracy of the integrated system was evaluated with phantom and intraoperative studies. It will now be presented the experimental protocol of both studies.

3.6.1 Phantom study

The 3DSlicer navigation system was running on the Mac laptop, the phantom was held by a Mayfield head frame attached to the operating table. Connected to the Mayfield frame there is the reference frame (blue) is present and the pointer used for measures (fuchsia colored) is shown close to the mac (Figure 3.20).

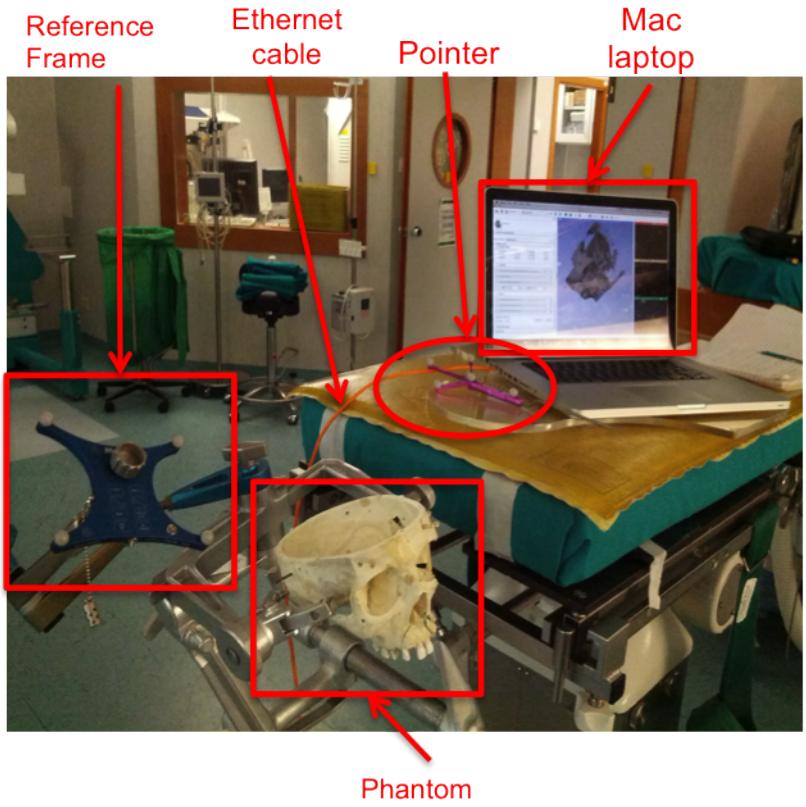

Figure 3.20: Phantom accuracy validation set-up. The phantom used for the experiments is held in the Mayfield frame that is connected to the reference frame (blue). The Ethernet cable was used for the connection to the Stealth-Station through the Hospital network. On the Mac laptop 3D Slicer is running and the CT of the phantom is loaded. The pointer was used to collect points for the experiments.

The study was performed with both registration modalities provided by the StealthStation (paragraph 3.1.4). The phantom was equipped with different landmarks visible in figure .

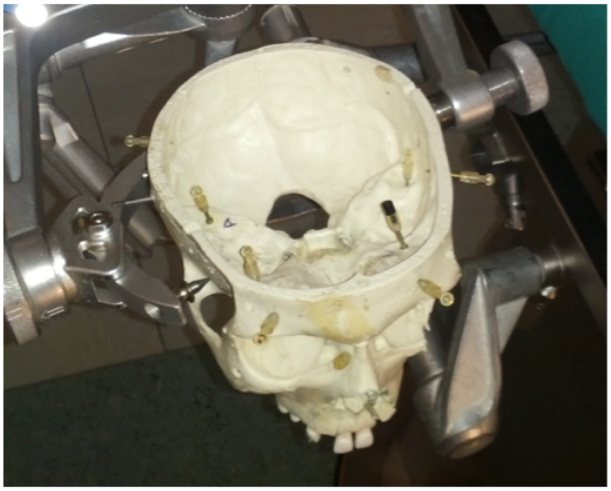

Figure 3.21: Fiducials markers used for testing the system accuracy.

All the 10 available fiducials were used for the experiments. The experimental protocol was:

1. Setting up-the the navigation in 3D Slicer activating the StealthStation navigator, the Windows client and the 3D Slicer module on the Mac laptop.

2. Pointing each fiducial landmark and storing 100 coordinates of the tool tip using the "Full Trajectory collection" function.

3. Selecting on a phantom 3D model (loaded in 3D Slicer) the location of each fiducial landmark for 3 times (Figure 3.22).

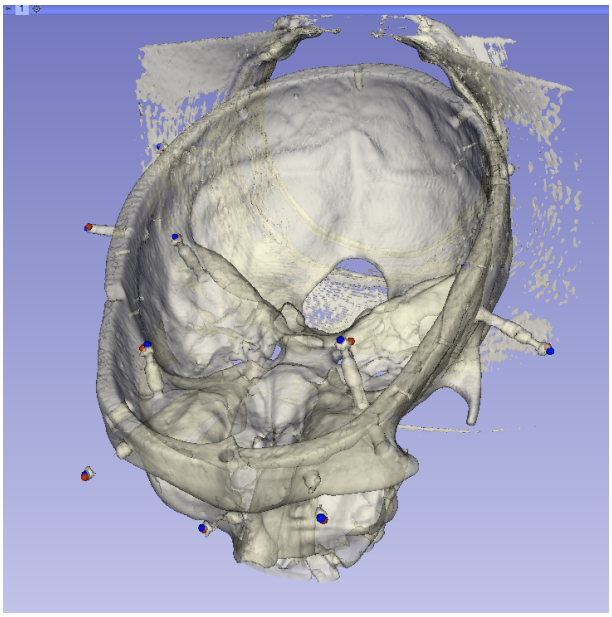

Figure 3.22: Points acquired in 3D Slicer: the blue dots represents points selected manually on the 3D model, the red point are stored with the integrated navigation system.

In Figure 3.22 the data acquired are shown on the phantom 3D model: Blue dots (Slicer Fiducial objects) are placed manually at the location of the landmarks. Red dots are placed automatically by the developed module at the pointer tip coordinates during the experiment. It is visible in the figure that there are little distances between points correspondent to each landmark. Those distances are used to estimate the Target Registration Error (TRE).

For the TRE computation data acquired were imported into Matlab and the following computation were performed:

- The 100 coordinates acquired for each fiducial location were averaged obtaining only 1 coordinates vector for each landmark.
- The 3 coordinate selected manually on the virtual 3D model were also averaged for obtain a single coordinates vector for each landmark.
- Euclidean distance between the two series of 10 coordinates vectors were performed.
- Median value and inter-quartile ranges were computed for the 10 Euclidean distances.

The experiment was repeated twice using different registration matrix (${}^{\mathbf{Image}}\mathbf{mm}\mathbf{T}_{\mathbf{Tip}}$) obtained from the StealthStation. Both StealthStation registration modalities (Tracer and PointMerge) were tested on purpose.

3.6.2 Patients fiducials accuracy

Intraoperative studies were performed in order to evaluate the system accuracy. Two patients subjected to resection surgery were chosen. Those patients previously underwent an intervention of Stereo Electro Encefalography (SEEG), an invasive diagnosis technique for identifying the epileptogenic zones [13]. The technique requires the insertion of depth electrodes that will then be removed after two or three weeks of monitoring. At the end of the procedure, a CT is performed in order to evaluate the accuracy of the electrodes positioning. This CT is then used for the creation of a 3D models of the electrodes that will be loaded on the 3D Slicer scene during the planning phase and also for the navigation. At the time of the resective surgical intervention the scars left by the electrodes are still visible on the skin and on the cortex. Those cortical scars have been used to evaluate the intraoperative navigational accuracy. In figure 3.23 (left) a picture of the cortex is shown, the letters (paper labels) are put in correspondence of the scars left by electrodes. In the right figure, the 3D Slicer scene with the electrodes visible and labelled with the same letters (T, B, I) are shown.

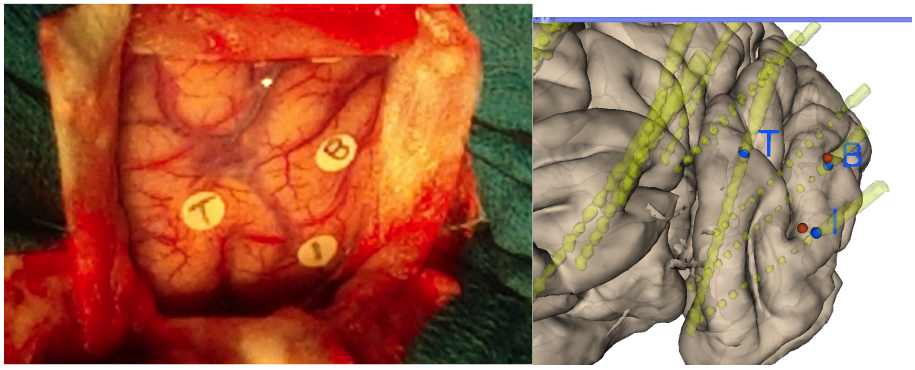

Figure 3.23: Real (left) and virtual (right) reality of the electrodes (scars) used for accuracy validation. Red fiducials are representation of the pointer tip acquisitions, Blue one are placed manually on the cortical model.

For this analysis the workflow was:

1. Surgeon positioning of the pointer on the electrodes left scars;
2. acquisition of the pointer tip in 3D Slicer through the **"Intraoperative annotation"** feature (Red fiducials in figure 3.23-left);
3. Surgeon removal of the pointer;
4. manual placing of Slicer fiducials in correspondence of each electrode location in the 3D Slicer model (Blue fiducials in Figure 3.23- right).

3 electrodes scars were acquired for each patient. The total number of acquisition performed was 6.

Data processing The pointer tip coordinates (Red fiducials) and the manually placed fiducials (Blue fiducials) were imported into Matlab for processing. The processing steps were:

1. Computation of the Euclidean distance between points acquired with the navigator and points placed manually;
2. Computation of the median value and inter-quartile ranges for the Target Registration Error estimation.

3.7 BrainShift analysis

Since brain shift is one of the main factor that compromise the navigational accuracy it was performed a study to evaluate quantitatively its extent. 7 surgical procedures were analyzed following the workflow in Figure 3.1.

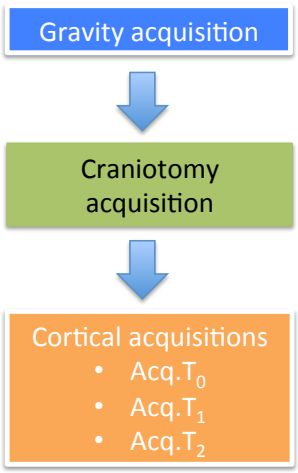

Table 3.1: Intraoperative acquisition protocol.

The **gravity direction** was obtained acquiring two vertical points (P1and P2) on a tripod (Figure 3.24) placed close to the patient.

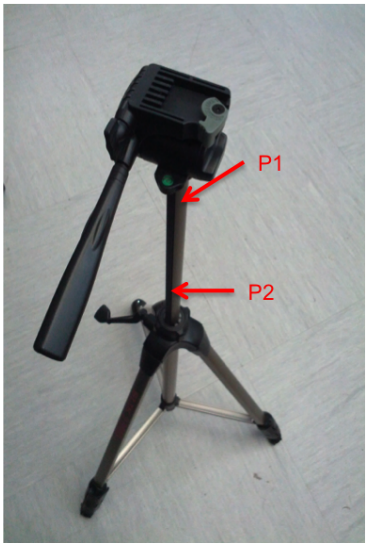

Figure 3.24: The photographic tripod used for vertical point intraoperative acquisition.

3.7.1 Craniotomy acquisition

The edges of the craniotomy were acquired using the sterile pointer and the "**Intraoperative annotation**" feature following the steps:

- surgeon pointing of a point along the edge of the performed craniotomy pointing on the dura mater;
- tool tip coordinates acquisition in 3D Slicer;
- surgeon removal of the pointer when the coordinates are stored;

The steps are repeated for all the 10-15 points necessary to obtain a sufficient approximation of the craniotomy edges. All the the process lasts no more than 2 minutes for each patient. Additionally the current time of the acquisition was saved for analysis ($T_{Craniotomy}$). In Figure 3.25 it is shown a patient craniotomy acquisition in the Slicer scene: the red dots are the intraoperatively acquired points.

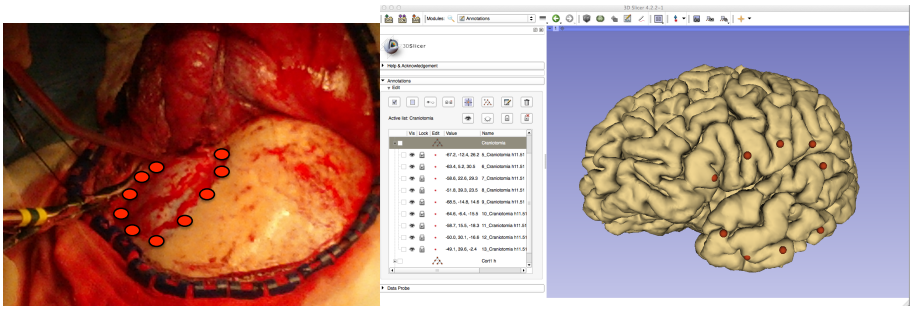

Figure 3.25: A craniotomy acquisition output in the 3DSlicer scene: red dots are the intraoperatively acquired points along the bone edge with the tool positioned on the dura mater surface.

3.7.2 Cortical points acquisition

The fundamental measures of the study are the cortical points coordinates. Three acquisition were made at the different surgery phases (dural opening $\mathbf{T}_0$, middle of the surgery $\mathbf{T}_1$, end of the surgery $\mathbf{T}_2$) with the following workflow:

1. after the dura mater opening the surgeon identifies some (N) fiducials points in the cortex. In this phase it is important for the surgeon to know in advance which cortical area will have been removed: the cortical points acquired must be the same in different acquisitions, this the area subjected to resection can not be considered for the analysis.

2. surgeon pointer positioning in the first identified point;

3. point is acquired with the Slicer navigator as soon as the surgeon confirms the stable positioning of the tool tip;

4. once the point is stored the surgeon can move to another point;

5. steps 2-4 are repeated for the N points;

6. the time of the first acquisition ($\mathbf{T}_0$) is saved;

7. at the end ($\mathbf{T}_2$) and during the surgery ($\mathbf{T}_1$), other two acquisitions were done repeating steps 2-6.

In Figure 3.26 the blue dots represent 6 cortical points acquired for a patient in the first time series (**Acq** $\mathbf{T}_0$).

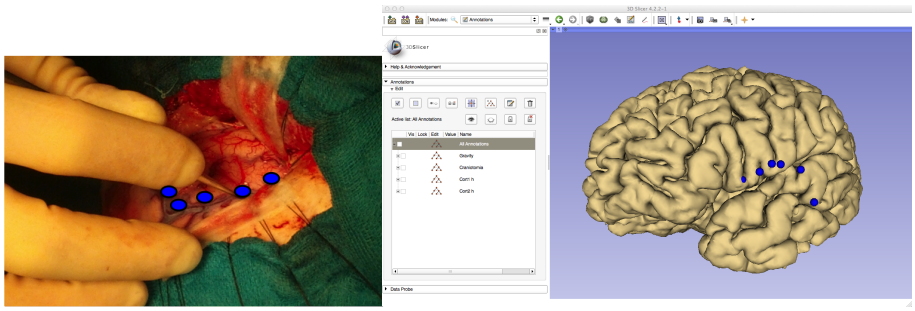

Figure 3.26: Slicer scene with 6 cortical acquired points.

In Figure 3.27 the same previous 6 points acquired at the end of the surgery ($\mathbf{Acq.T}_2$) are represented in red. The pial surface model has been shaded in order to show that the points collected shifted in the inward direction during surgery.

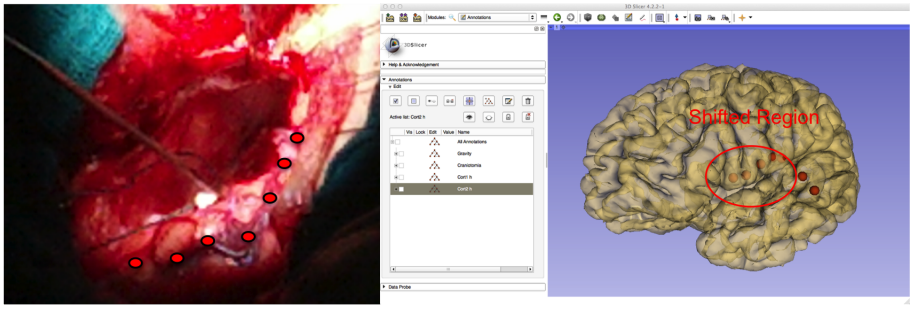

Figure 3.27: The last acquisition of the 6 cortical points. It is clearly visible how the points acquired shifted in the inward direction during surgery.

3.7.3 Brain shift Data analysis

In the following paragraphs the methods used to estimate the bran shift from the acquired points will be outlined. First of all the vectors used for analysis are defined.

Definitions The vectors representing the shift are defined as follows:

$$\mathbf{SV1}(i) = \mathbf{Acq.T_1}(i) - \mathbf{Acq.T_0}(i), i = i...N \tag{3.6}$$

$$\mathbf{SV2}(i) = \mathbf{Acq.T_2}(i) - \mathbf{Acq.T_0}(i), i = i...N \tag{3.7}$$

$$\mathbf{SV3}(i) = \mathbf{Acq.T_2}(i) - \mathbf{Acq.T_1}(i), i = i...N \tag{3.8}$$

Where $\mathbf{Acq.T_0}$, $\mathbf{Acq.T_1}$ and $\mathbf{Acq.T_2}$ are vectors of points defined in paragraph 3.7.2 and N is the number of cortical points acquired for the patient.

The gravity direction versor ($\mathbf{g}$) was computed as:

$$\mathbf{g} = \frac{\mathbf{P2} - \mathbf{P1}}{\|\mathbf{P2} - \mathbf{P1}\|} \tag{3.9}$$

where P2 and P1 are the points acquired in the gravity acquisition and $\|\cdot\|$ is the quadratic norm of the vector and N is the number of cortical points acquired for the selected patient.

The craniotomy normal vector ($\mathbf{n}$) is defined entering the patient head. It was computed through a VTK function that computes the plane approximating the points obtained with the craniotomy acquisition. The output of the VTK function is the plane shown in figure 3.28.

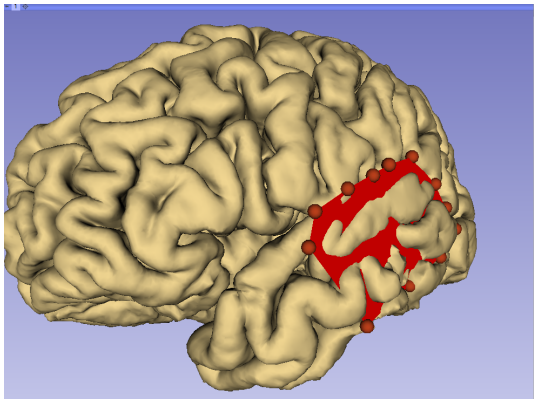

Figure 3.28: VTK Polygon created with the points collected for the craniotomy acquisition.

In Figure 3.29 a schematic representation of all the defined vectors in shown.

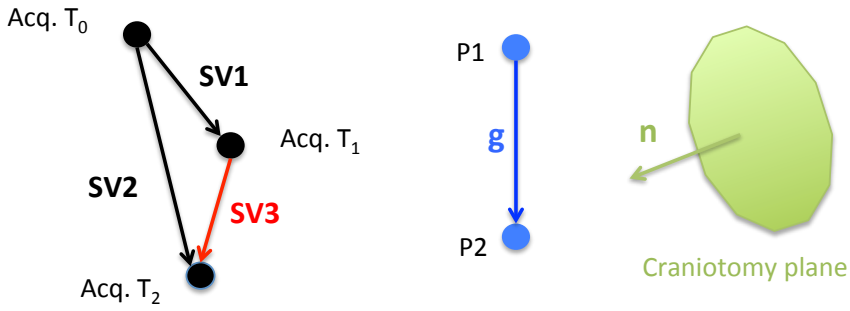

Figure 3.29: Vectors definitions. From left to right: Shift vectors for cortical acquisition, gravity vector, and craniotomy normal vector.

Shift estimation The defined vectors were computed for all the acquired points exporting the Slicer coordinates in Matlab®. For the shift estimation the modulus of **SV2** was computed. When $\mathbf{Acq.T_1}$ was available also the module of **SV1** was computed. Medians and interquartile ranges of shift vectors were computed for each patient.

Method to compute angles In order to analyze to what extent brain shift occurs in the gravity direction the following formula has been used.

$$\alpha(i) = \arccos \frac{\mathbf{SV2}(i)\cdot\mathbf{g}}{\|\mathbf{SV2(i)}\|}, i = 1, ...N \tag{3.10}$$

Where $\mathbf{SV2}(i)\cdot\mathbf{g}$ is the scalar product between the two vectors. The formulae have been derived as the inverse of the scalar product definition considering that $||\mathbf{g}||$=1.

$$\mathbf{SV2}(i)\cdot\mathbf{g} = \|\mathbf{SV2(i)}\|\|\mathbf{g}\| \cos\alpha \tag{3.11}$$

with α angle between the two vectors.

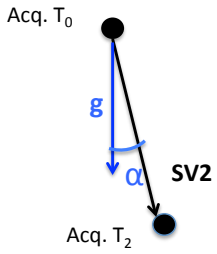

Figure 3.30: Definition of the α angle: angle between the shift vector and the gravity vector.

For the analysis of angle between $\mathbf{n}$ and the shift vector formula 3.12 has been used:

$$\beta(i) = \arccos \frac{\mathbf{SV2}(i)\cdot\mathbf{n}}{\|\mathbf{SV2(i)}\|}, i = 1, ...N \tag{3.12}$$

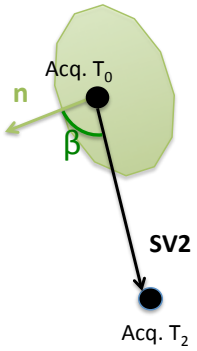

Figure 3.31: Definition of the β angle: angle between the shift vector and the craniotomy plane normal vector.

Medians and interquartile ranges of both angles where computed.

When it was available also the intermediate cortical acquisition ($\mathbf{Acq.T_1}$) also the angle between **SV1** and **SV3** was computed using the formula 3.13. The angle was computed in order to evaluate the consistency of the shift direction during time. A full consistency in the direction would lead a null angle between the two vectors ($\gamma = 0 \Leftrightarrow$ **SV1**//**SV3**)

$$\gamma(i) = \arccos \frac{\mathbf{SV1}(i) \cdot \mathbf{SV3}}{\|\mathbf{SV1(i)}\| \|\mathbf{SV3i)}\|}, i = 1, ...N \tag{3.13}$$

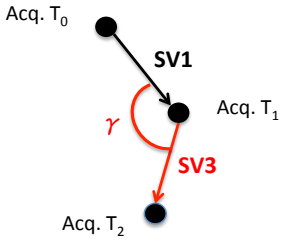

Figure 3.32: Definition of the γ angle: angle between consecutive shift vectors.

Finally the orientation of the craniotomy has been computed as the angle between **n** and **g. The following formula has been used:**

$$\vartheta(i) = \arccos(\mathbf{g} \cdot \mathbf{n}), i = 1, ...N \tag{3.14}$$

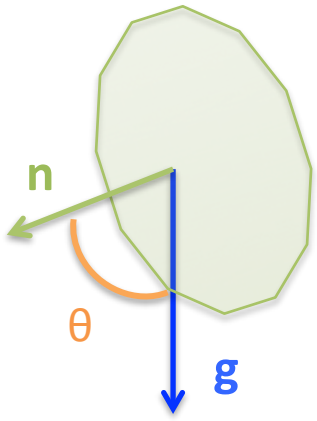

Figure 3.33: Definition of the θ angle: angle between the craniotomy normal and the gravity vector. It is used to estimate the orientation of the craniotomy.

Correlations of the θ angle and the craniotomy surface area with the brain shift ($||\mathbf{SV2}||$) were perfomed through the Pearson[25] method. The craniotomy surface area was obtained as the polyghon surface returned by VTK.

Chapter 4

Results

In this chapter the result of the system, accuracy evaluation and the brain shift analysis are presented.

4.1 System accuracy

Results of the system accuracy study are shown in Figure 4.1.

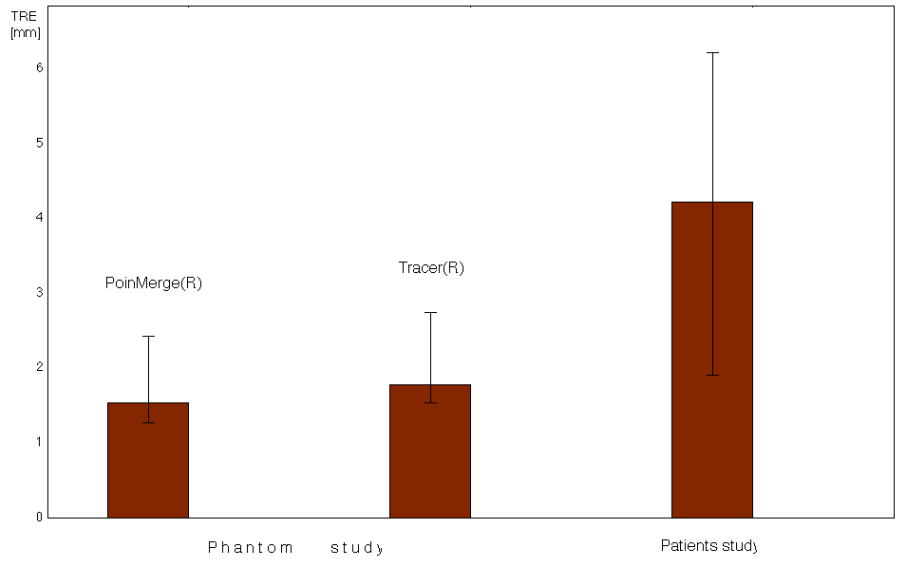

Figure 4.1: System accuracy study

In the abscissa results are divided for the Phantom and Patients Study, in ordinates there is the TRE expressed in millimeters. The phantom study is

divided in two: the first block is the result of the analysis performed with the PointMerge registration method and the second is the one performed with Tracer registration method. It is clearly visible the difference between the phantom and the patients study accuracy and as expected the point to point registration method reached an higher accuracy (i.e lower TRE) even if the difference is little. Patients study presents higher interquartile ranges and the TRE is much higher than phantom studies. In table 4.1 the result are summarized.

	Phantom		**Patients**
	TRE[mm]	FRE[mm]	TRE[mm]
PointMerge®	1,53	1,39	/
Tracer®	1,72	/	**4,21**

Table 4.1: System accuracy: TRE and FRE computed for each study are shown.

The acquisitions performed for a patient are shown in figure 4.2. Blue dots are placed manually at the electrodes location, red dots are placed with the navigator.

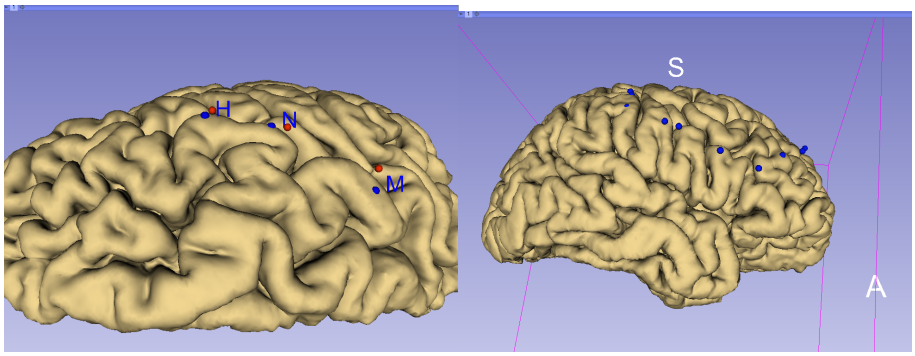

Figure 4.2: Left image: a patient electrodes position measures (red dot), and electrode location in the image (blue dots).

4.2 Brain shift results analysis

In this section, results of the preliminary study about brain shift estimation using the presented system, are outlined.

4.2.1 Data collected

As mentioned before, 7 surgical procedures were included in this study. In Table 4.2 each procedure is identified by Patient ID that will be used as a tag for the analysis. All the analyzed surgeries are resections in patient with drug resistant epilepsy. The epileptogenic pattern describes the area of the brain from which

the epileptogenic foci are generated. The resections are of type: cortectomy, lobectomy (if the entire lobe is resected) or lesionectomy (when only the lesion is removed). The last column is referred to the patient orientation during surgery, it is computed as described in paragraph 3.7.3.

Patient ID	**Epileptogenic Pattern**	**Surgery Type**	**Craniotomy orientation, θ (°)**
1	Temporal lobe	Lobectomy	40.12
2	Temporal cortex	Lesionectomy (DNET*)	21.83
3	Temporal cortex	Lesionectomy	36.65
4	Temporal lobe	Lesionectomy/Cortectomy	50.53
5	Temporal cortex	Cortectomy (SEEG)	48.41
6	Temporal Cortex	Cortectomy(SEEG)	39.65
7	Temporal	Lesionectomy	48.18

Table 4.2: List of patients with their epileptogenic pattern, surgery type and patient orientation θ 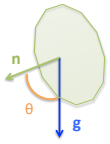

. *Dysembryoplastic neuroepithelial tumor.

For each patient, different acquisitions with the developed navigator were performed. Those acquisitions are summarized in Table 4.3 detailed for every patient. The first column reports the number of points acquired for each acquisition series and the second reports the number of acquired series. The last column represents the elapsed time between acquisition: the first sub-column is the time (in minutes) between the craniotomy acquisition ($T_{Craniotomy}$ chosen as "zero shift" time reference) and the first cortical acquisition ($\mathbf{Acq.T_0}$), the second is the time between $\mathbf{Acq.T_1}$ and $\mathbf{Acq.T_0}$, the third (when present) is the time between $\mathbf{Acq.T_2}$ and $\mathbf{Acq.T_1}$. A total of 36 cortical points were analyzed.

Patient ID	**#Points**	**#Series**	**Time [min]**		
			$T_{Craniotomy} - T_0$	$T_1 - T_0$	T_2-T_1
1	4	3	20	80	131
2	6	3	32	89	130
3	7	3	29	116	74
4	6	2	28	100	/
5	3	2	71	126	/
6	4	2	94	280	/
7	6	2	40	210	/

Table 4.3: Cortical acquisition data. The first column represents the number of point acquired for each acquisition series (N), the second represents the number of acquired series (2 or 3). If the number is 2, it means that one acquisition has been performed at the beginning of the surgery and one at the end, if 3 an intermediate acquisition has been done. The last column represents the elapsed time between acquisitions in minutes.

4.2.2 Time influence result analysis

Time influence on brain shift is shown in the chart of Figure 4.3. Time referenced to $T_{Craniotomy}$ is represented in abscissa, the median shift is represented in ordinates. Patients are represented by different colors. Squares represents samples. The first sample correspond to the $\mathbf{Acq.T_0}$ (reference), the second to $\mathbf{Acq.T_1}$, the third to $\mathbf{Acq.T_2}$. Error bars represents the interquartile ranges (0.25-0.75).

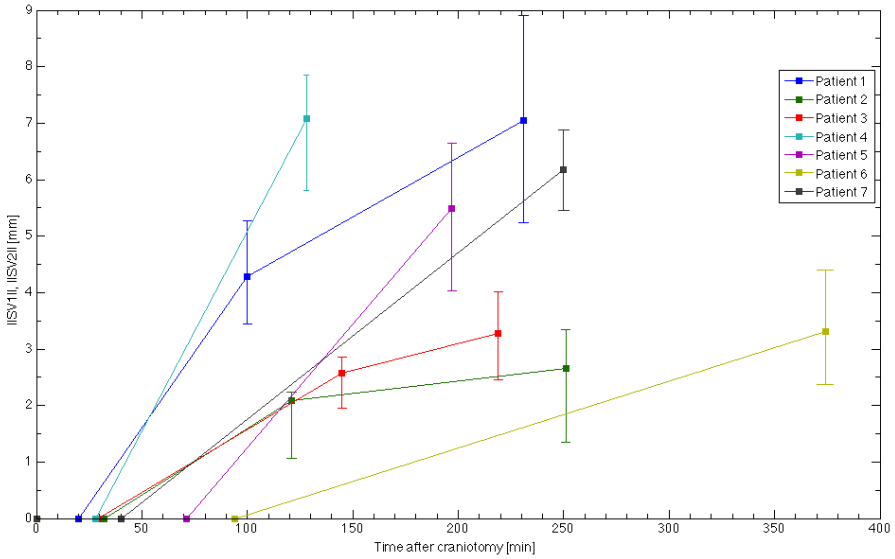

Figure 4.3: Time influence on brain shift: each patient is represented by differently colored curves. The shift is represented in ordinates, time in abscissae, samples are represented by squares. Each sample is the median value of the shift of all the patient collected points, the error-bars represent the inter-quartile (0.25 - 0.75) range.

The only patients that encounter a shift greater that the TRE (4,21 mm) are Patients 1,4,5 and 7 (Figure 4.4). **Patients 2,3 and 6** will be analyzed in more detail and discussed.

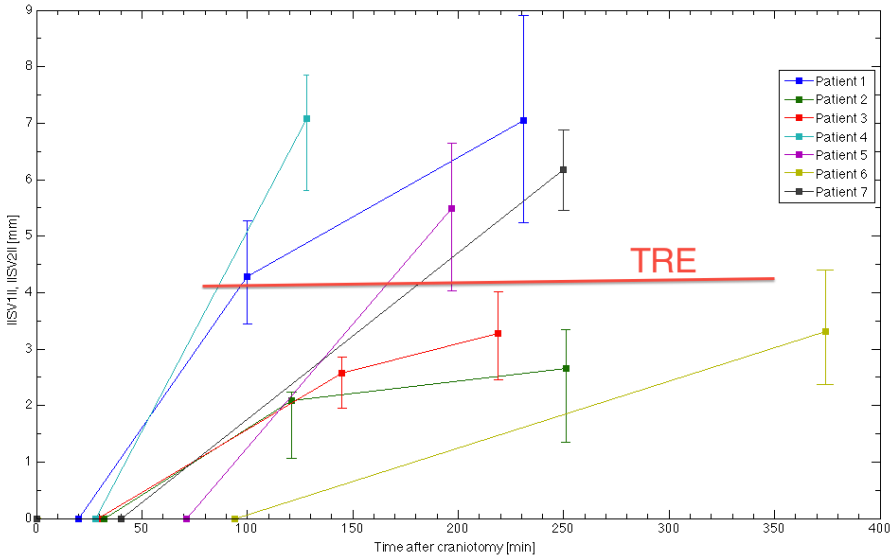

Figure 4.4: TRE used as a threshold for the study reliability. The shift is represented in ordinates, time in abscissae, samples are represented by squares. Each sample is the median value of the shift of all the patient collected points, the error-bars represent the inter-quartile (0.25 - 0.75) range.

4.2.3 Shift Directions results analysis

In Figure 4.5 the height of the blue bars represent the median angle between the shift and the gravity direction (angle α defined in equations 3.10). The green ones represent the median angle between the shift and craniotomy plane normal (angle β, defined in equation 3.12).

The median α angle is 34° (red dotted line), the median β is angle is 50°.

Error bars represent the first and third quartile. **Patients 2, 3 and 6** has the greater interquartile ranges for both angles: they will be discussed in section 4.2.3.2. Two of them will analyzed in more detail in section 4.2.3.1.

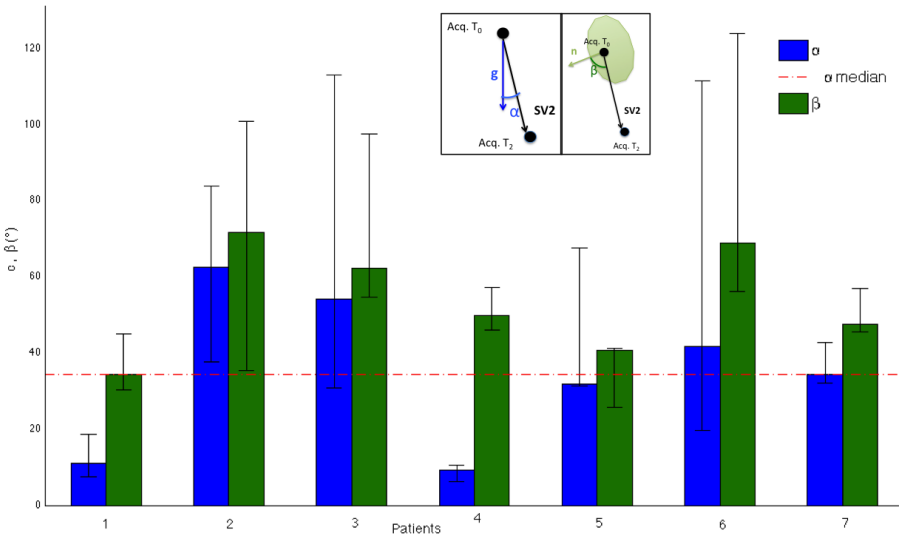

Figure 4.5: Brain Shift direction analysis results. Blue bar represents the median angles between gravity and shift vectors , green one the median angle between normal of the craniotomy plane and shift vectors . Error bars are the interquartile ranges. Red dotted line is the median gravity angle of the patients analyzed.

4.2.3.1 Shift Direction consistency

For patients with 3 acquisition series (**Patients** 1**,2 and 3**, Table 4.3) it has been possible to perform a deeper analysis: the individual study of two independent shift vector (**SV1** and **SV2** defined in 3.63.7) with respect to **SV3** (defined in 3.8). This extra analysis has been performed for understanding the reason of the previous results regarding **Patients 2 and 3**. In figure 4.6 the angle γ of the three patients analyzed is shown. A big difference is shown between patient 1 and patients 2,3. Patient 1 has an angle close to 0, the other patients have angles of about 90°.

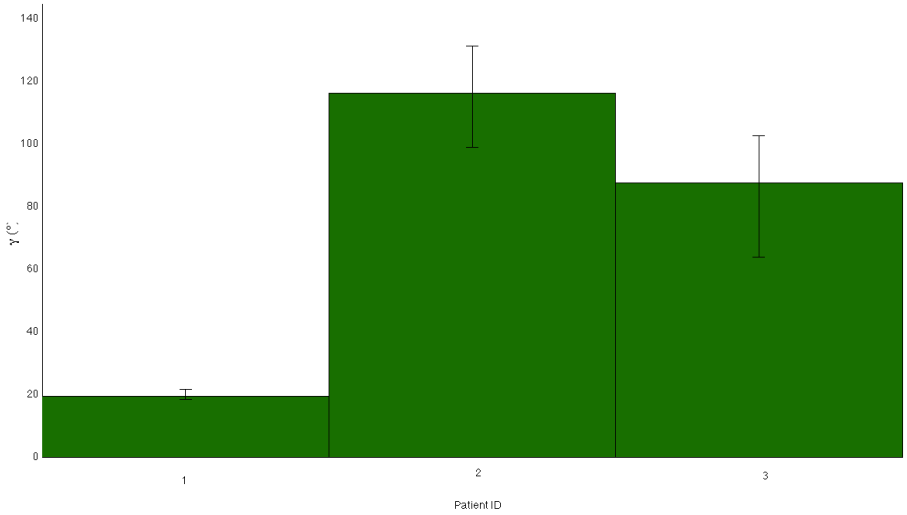

Figure 4.6: Patient 1,2 and 3 shift direction consistency analysis. The angle γ computed by formula 3.13 is low only for patient 1.

4.2.3.2 Patients 2, 3 and 6 analysis

As said Patients that have been excluded by the TRE consideration and that presents high interquartile ranges in the directions analysis will be analyzed in detail. The data collected for patient 2 are shown in Figure 4.7. The left figure is a picture of the brain taken at the time of the first acquisition of points. The six points acquired are marked by green circles. In the corresponding virtual reality (3D Slicer scene, at the right) are visible the 6 acquired locations. The first three points at the top of the figure are highlighted (P1,P2, P3) because this analysis will be focused on those three points.

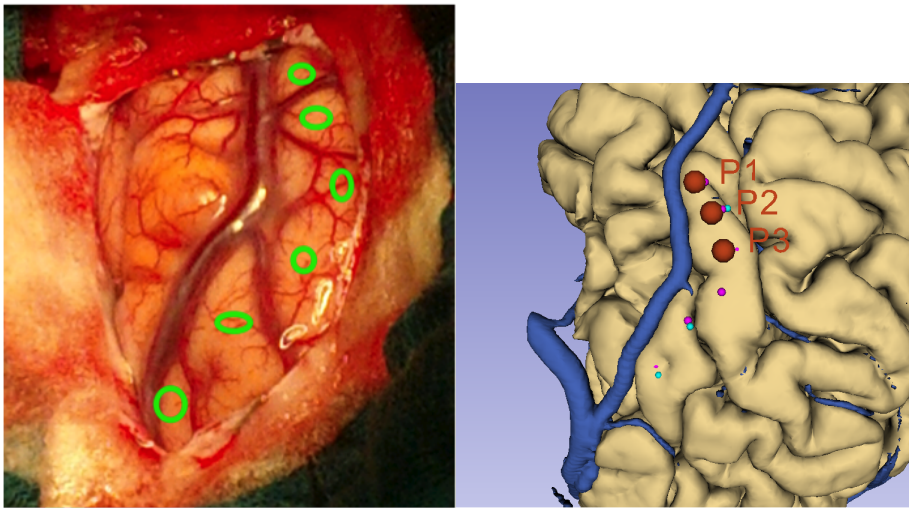

Figure 4.7: Patient 2 landmarks collected (left). 3D Slicer scene with the corresponding landmarks (right). P1, P2 and P3 are in particular the one used for this analysis.

The following table shows the module of **SV2** for three points with is its module (distance between points) and its angle with respect to gravity (α). First of all it has to be noted that the shift modulus are always smaller that the TRE (4,21 mm), but it can be noted that the shift module and the gravity angle is growing from P1 to P3. This results could suggest that the main shift could have been happened in the vicinity of P1. The fact that gravity angle is inversely proportional to the shift module could be interpreted as inaccurate repositioning of the surgeon in the same point. For P3 for example shift did not occurred (0.67 mm) thus the vector considered as brain shift is actually only the difference of the two acquired positions of the "same" point.

	$\|\|\mathbf{SV1}\|\|$ [mm]	α[°]
P1	2.01	31.0
P2	1.06	51.7
P3	0.67	76.6

Table 4.4: Result of the analysis of the three most significant points.In this case the the bigger is brain shift the lower is the angle with gravity. Big angles due to the absence of brain shift change the statistics enlarging the interquartile range in Figure 4.5.

In Figure 4.8 it is displayed a picture taken at the end of the surgery. It is clearly visible that the main shift occurred at the top of the craniotomy where a green arrow is shown. The 3 points analyzed are close to the main shift region and P1 is the closest.

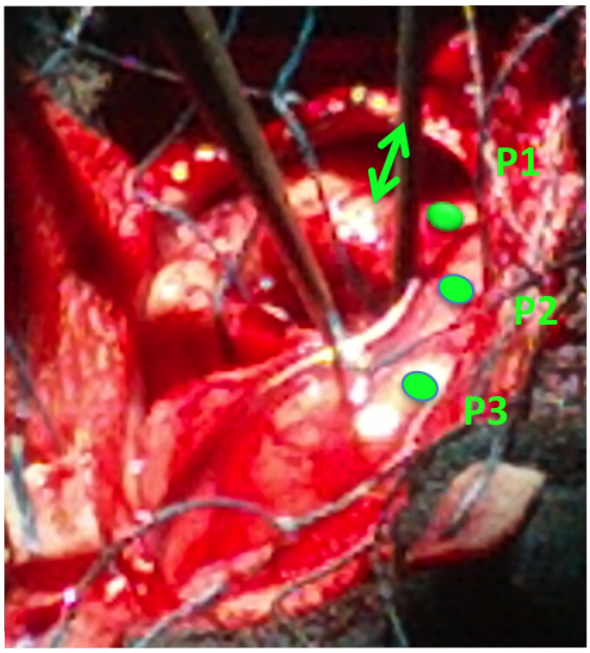

Figure 4.8: End of surgery condition: the arrow points where the main shift occurred. In green the points used for the analysis.

Patient 3 has also been analyzed in detail. For this patient 7 points have been acquired 3 times. The three points that mainly were subjected to brain shift are highlighted in Figure 4.9 (right).

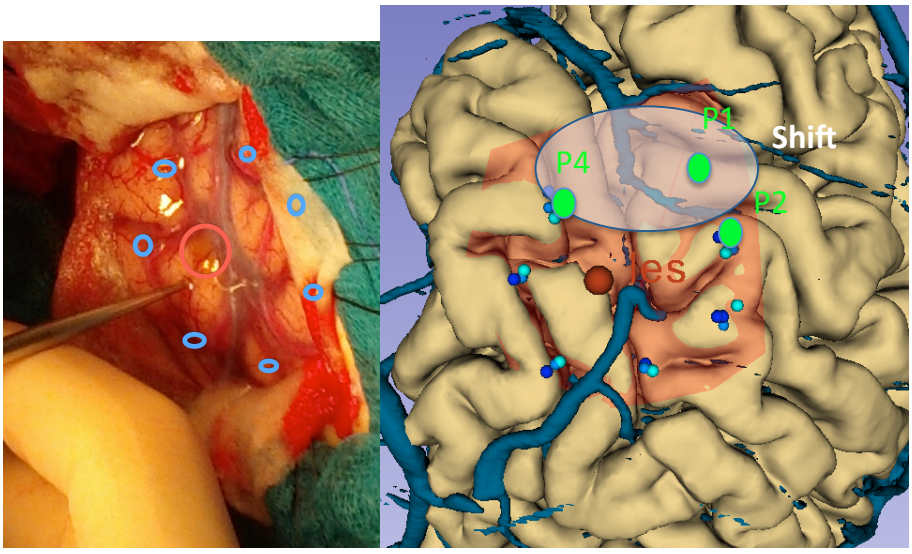

Figure 4.9: Points collected intraoperatively for Patient 3. Only the upper three points (green) will be used for this analysis.

In the following table the two shift vectors are analyzed separately, (**SV1** and **SV2**). The most significant shift (in magnitude) in that case happens in the third acquisition phase (SV2). In both case we note that angles with gravity for this points are always less than the median value of the patient explaining the reason of the high inter-quartile range (Figure 4.5).

	||**SV1**|| [mm]	α[°]	**SV2**[mm]	α[°]
P1	2.6	14.3	3.79	27.8
P2	3.9	46.9	3.27	33.1
P4	2.6	20.3	4.37	46.0

Table 4.5: Detailed analysis of the shift magnitude and direction (angle with gravity). For these three points the angle with gravity are little demonstrating to be real shifted points. The 4 points acquired that were not subjected to brain shift are the responsible of the big interquartile ranges of figure 4.5.

In Figure 4.10 postoperative shift is visible and the locations of the analyzed points are highlighted.

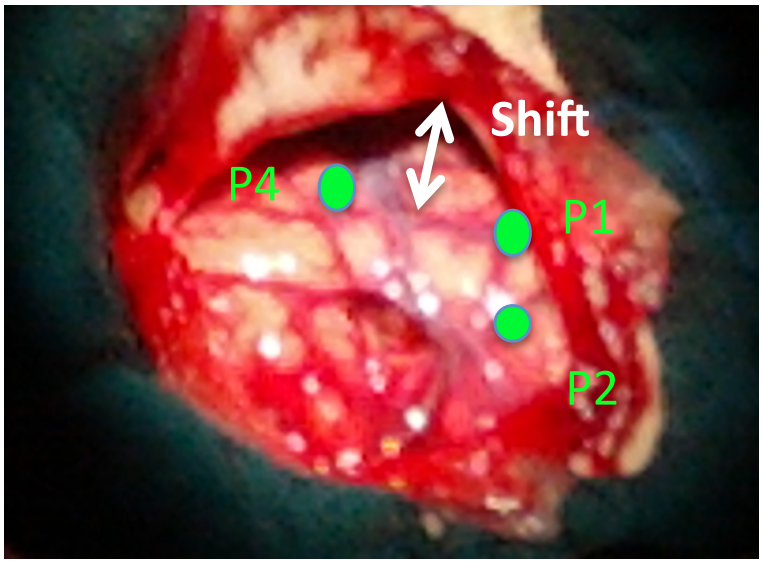

Figure 4.10: Postoperative picture of patient 3. The shift is clearly visible in the upper part of the craniotomy. Green dots are the analyzed landmarks.

The last patient to be analyzed is Patient 6. This was a patient that underwent a SEEG procedure, in Figure 4.11 there is the Slicer scene of the patient with the craniotomy model created with the "Craniotomy" feature of the navigator. Electrodes locations are identified by letters (H, N, M) and the points chosen for the analysis are labelled with the name (H, P2, P3, P4). At the right side of the picture it is shown the postoperative condition with the same landmarks of before. From the picture it is evident to see that shift occurs at the left side (white circles).

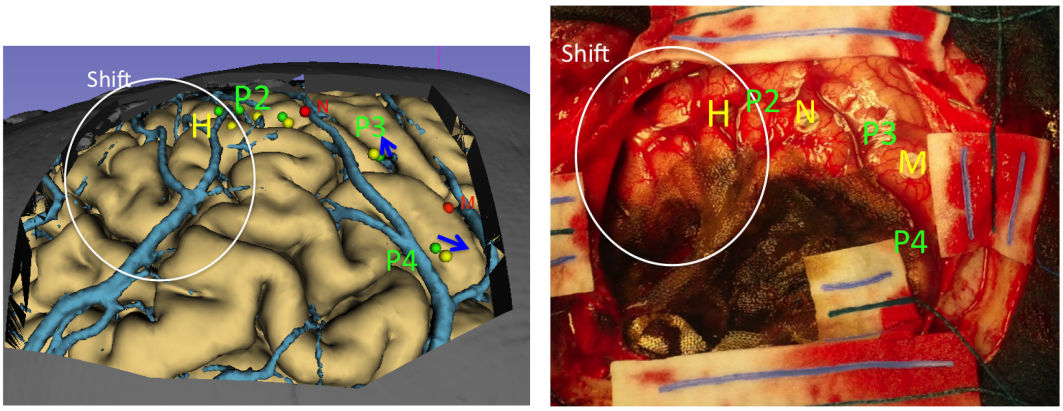

Figure 4.11: Intraoperative acquired points. Green dots in at the left side are taken in the first acquisition, and yellow ones are the last acquired. H is an electrode used as landmark and analyzed with P2, P3 and P4. In that case shift occurred in the opposite direction in different cortical area.

In the following table Shift modulus and angles between gravity are represented. It is interesting to note that points H and P2 has a little angle with gravity, P3 and P4 instead have angles greater that 90°, which means that those points (far away from white circle region) had been subjected by an antigravitary shift. This result can be confirmed also visually checking the direction of the shift in Figure 4.11: green dots are the first acquisition series, yellow dots are last acquisition series. Shifts in the locations H and P2 point in the brain inward direction and ones corresponding to P3 and P4 fiducials points in the outward direction (blue arrows).

	$\|\|\mathbf{SV2}\|\|$[mm]	α[°]
H	4.63	12.8
P2	4.32	21.9
P3	3.31	96.6
P4	2.61	156.7

Table 4.6: Points used for the analysis. Clearly points H and P2 shifted in the gravity direction, and P3, P4 in the "opposite" direction.

This analysis showed why the inter-quartile ranges of Figure 4.5 for the selected patients are so extended. The statistical analysis could in fact be considered feasible only for patient with a cortical homogeneous shift.

4.2.4 Brain Shift correlation with the craniotomy extension

The last performed analysis was the correlation between brain shift and the area of the craniotomy. The chart in Figure 4.12 shows the scatter plot of the registered values: brain shift data are the same of Figure 4.3 (median values). The label close to every square represents the patient number.

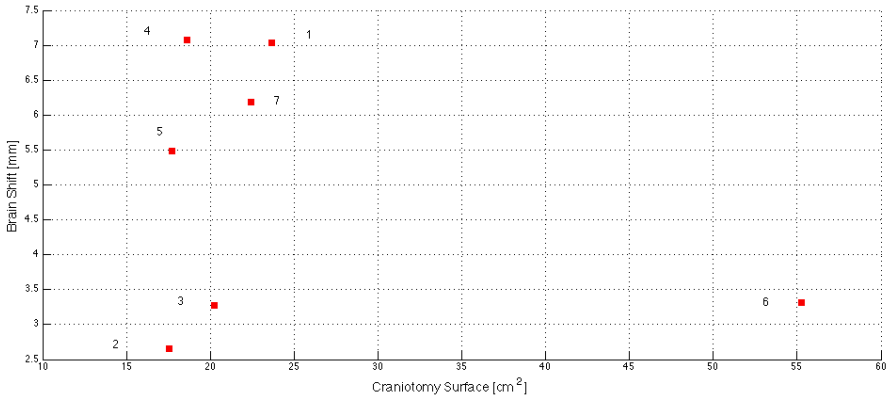

Figure 4.12: Brain shift VS Craniotomy surface plot. Every point represents the patient value corresponding to the label. Patient 6 could be considered as an outlier because its craniotomy was two times greater that the average.

A linear interpolation has been found considering the sixth patient as an outlier because its craniotomy surface is more than the double of the average value. The regression is displayed in Figure 4.13. The upper chart represent the data from patients 1,2,3,4,5 and 7 fitted by the linear regression with equation $BrainShift = 0.36 * CraniotomySurface - 1.9$. The Pearson correlation test returned a correlation value of 0.4814, with a p-value of 0.3337. No correlation was found between variables.

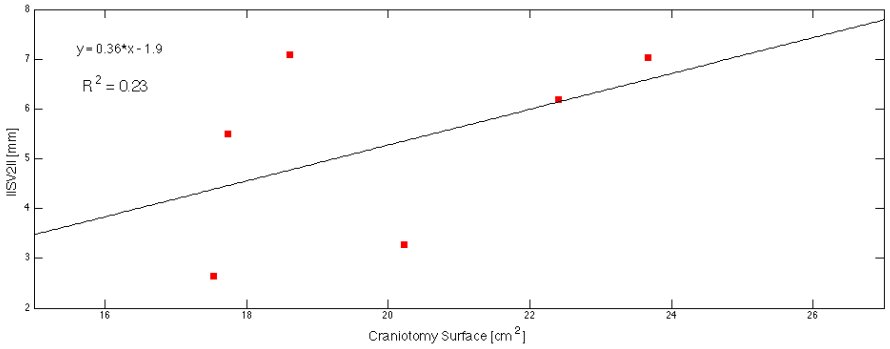

Figure 4.13: Linear regression of data in Figure 4.12 (excluding patient 6).

4.2.5 Brain Shift correlation with the craniotomy orientation

The last analysis showed in Figure 4.14 shows the linear regression between brain shift and the orientation of the performed computed by formula 3.14. Coefficient of determination is $R^2 = 0.5486$. The Pearson correlation test returned a correlation value of 0.7578, with a p-value of 0.0484. The two variable resulted thus correlated.

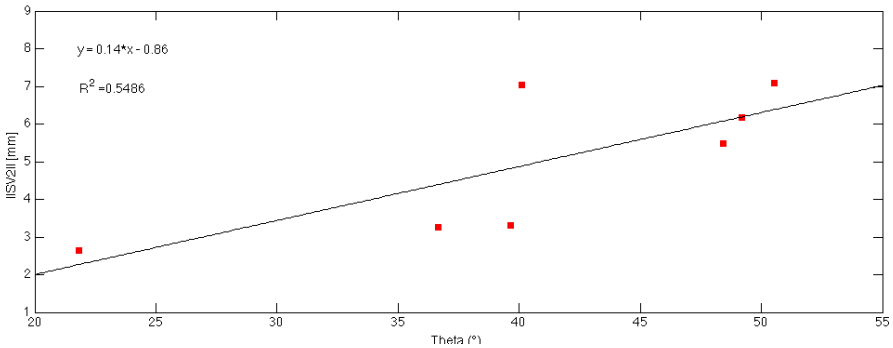

Figure 4.14: Linear regression of craniotomy orientation and brain shift data.

Chapter 5

Discussions

In this chapter an overview of the qualitative outcomes had with the developed integrated system will be first of all highlighted. Then the results about the system accuracy and the feasibility study for brain shift estimation will be analyzed in detail.

5.1 Integrated system acceptance

The clinical acceptance of the system was facilitated by the fact that surgeons of the Niguarda team are already familiar with the 3DSlicer environment. The system integration augmented in a considerable way the virtual reality environment available for navigation because 3D Slicer is a much more powerful visualization tool than the StealthStation Cranial software available at Niguarda center.

The system integration significantly improved the original system in different surgical situations. The system was particularly appreciated during interventions on patient that previously underwent SEEG . In this situation it is fundamental for surgeons the correct localization of implanted electrodes. In order to easily do this procedure, the common technique is to manually define the entry and target points of the electrodes in the exams loaded in the StealthStation® prior to surgery using a dedicated station's interface. This information is then used during navigation for identifying the navigated electrode location. With the new system it is not necessary anymore to define manually the electrodes location, that requires time, because the electrodes models are already present in the navigated 3DSlicer scene.

Furthermore the system does not substitute the original one, but it is just additional. Tracking data are in fact obtained from the StealthStation®, without affecting the system: all the original functionalities are absolutely maintained.

The standard use of the navigator does not require any user intervention except from the initialization phase. For using other functionalities instead it is required a user interaction: those functions has been added in order to augment the virtual reality environment and the possibility to add and store

useful intraoperative information.

It has been verified that the system is robust to the changing of the tracked tool: during surgery at least once the tool is changed (from non sterile to sterile one) .The tool calibration matrix is in fact accessed continuously together with all the other dynamic information: frame transform, tool transform, and the registration transform. Actually the latter should not be considered as dynamic but, its continuos access has been done in order to augment the system usability. If this information would have been retrieved only at application start-up the user should have been aware to start the application only after the registration process is finished on the StealthStation. In clinical situation it is better to have the smallest possible complications and so, with this solution the user is free to start-up the application even before the registration is performed.

Of course the system has also different limitations. One of the most important is the fact that it is not possible to command it directly from the operating theater in the sterile field. The limitation is in general particularly annoying also for the management of the normal 3D Slicer interface (i.e. changing the view of the pial model, set object visibility, navigate between exam slices). The Medtronic navigation has instead a special foot switch that can be pressed by the surgeon in sterile situations. Having a similar possibility would improve the system usability for example connecting the foot switch pressed event to the freezing functionality of the "navigator" module.

5.2 Accuracy evaluation

The results obtained for the patients fiducials accuracy study will now be analyzed.

	Presented Study	Shamir, 2008[29]	
	TRE[mm]	TRE[mm]	FRE[mm]
PointMerge®	/	4.1±1.6	3.9±1.2
Tracer®	4,21	/	/

Table 5.1: Comparison of the result obtained with a StealthStation accuracy study.

In Table 5.1 the accuracy result obtained in section 4.1, in particular the TRE obtained from the patients study, is compared with the study of Shamir et al. 2009[29]. The difference between the studies are:

- Shamir used the point to point registration procedure;
- Shamir analyzed 612 observations;
- Shamir computes also the clinical Fiducial Registration Error (FRE).

The difference of the sample size between the presented study and [29] suggests a deeper investigation in order to make the results comparable. In fact the

variability range of the presented study results is high. This is due the fact that there was significant difference between the accuracy obtained for the two patients analyzed. The first patient obtained a median TRE of 6,21 mm because the first acquisition has been taken when an important brain shift already occurred (even if it was not possible to measure it with this set-up). For the second patient instead the first acquisition has been taken in a zero brain shift condition leading to a median TRE of 1,90 mm.

It is possible to have an idea of the non measured brain shift looking at the Figure 4.2. Red dots are intraoperative measures of electrodes locations: the fact that they are so far away from the cortex means that the real cortical surface shifts occurred before the measures. This error is not due to mis-registration. It has in fact been verified that the points acquired 90 minutes before on the dura mater were lying in the proximity of the 3D model cortical surface as expected (Figure 4.2 right).

In any case it has been decided to consider also the first patient for the TRE computation because intraoperative TRE should take into account also brain shift problematic.

The FRE computation was not possible in this study because a surface registration methods was used clinically.

5.3 Brain shift study

5.3.1 Time influence

The first result is the one about time influence for brain shift. The chart in Figure 4.3 shows that brain shift varied for the patient between 2 to 7 mm (median values). From the results obtained in Table 5.1 the clinical patient accuracy of the system is 4,21 mm. Brain shift, lower than this threshold should not be considered as a valid measure. The clinical TRE in fact takes into account also the accuracy that a surgeon may have in repositioning the pointer tip in the same position. Considering the intraoperative TRE as a threshold for data validity leads to an exclusion of patients **2,3,6**, because of their non relevant brain shift. Only patient 1,4,5 and 7 should therefore been considered valid for the brain shift analysis (Figure 4.4).

5.3.2 Directions Analysis

Also the results about shift direction analysis need to be evaluated. The first important thing is that it has been found that gravity is the predominant shift direction with a median angle α between the shift of all patients of 34.4° considered a little deviation with gravity, confirming the state of art [26]. The median angle of the craniotomy (β) is instead 50°. It is worth to note how the patients present different behaviors for those variables. **Patients 2, 3 and 6** presents big interquartile ranges thus the angles (α and β) are very dispersed and also the median values are greater than the overall median (red line for α).

Interestingly those patient **are the same** excluded by the previous analysis for non having evident brain shift. At this point those patients need to be analyzed in detail and for this purpose a revision of the data collected has to be done. Furthermore the deeper analysis made in section 4.2.3.2 for those patients shows that in case that brain shift did not occur homogeneously the analysis statistical analysis performed was not feasible.

5.3.2.1 Shift consistency for Patients 1,2,3

As mentioned for patients 1,2,3 it has been possible to better analyze the shift evolution during surgery (Figure 4.6). Results from patient 1 confirms the intuitive assumption that **shift direction does not change during the surgery.**

Results from patients 2 and 3 are not consistent. Those patients were already been excluded by the first statement about threshold of acceptable brain shift (Section 5.3.1). This result reinforces the initial statement: the fact that the angle between **SV1** and **SV3** (γ) is nearly 90° is physiologically unacceptable. The points studied did not shift at all during surgery, or the shift occurred is not measurable with this set up.

5.3.3 Brain Shift correlation with craniotomy area and craniotomy orientation

It is now discussed the result regarding the correlation between the craniotomy extent and the brain shift. In chart in Figure 4.13 it was performed a linear correlation of the data considering the patient 6 data as an outlier. Confirming the state of the art [27] from the results it can be stated that there is not correlation between the variables.

A correlation of brain shift with the patient (its craniotomy plane) orientation was instead found.

Chapter 6

Conclusions and future work

In this chapter some conclusions about the project described in this thesis and possible future works will be given. In the first two sections is discussed the main objective reached by the system integration and the main limitations of the proposed study for brain shift estimation.

6.1 Integrated system

The system proposed has been shown to be used in clinical procedures in addition to the original StealthStation navigator (Medtronic system). Its improvements with respect to the original system could be summarized as follows:

- multimodality of the navigated data: coregistered MRI, FLAIR, CT, fMRI, DTI and 3D model obtained with one of the better performing cortical and white matter segmentation tool available at the moment (FreeSurfer);
- real-time navigation;
- intraoperative annotation feature, that allow the surgeon to annotate navigated location for intraoperative or post-operative analysis;
- advanced 3D graphics tool for augmenting the virtual reality of the navigation scene (craniotomy/durotomy visualization);
- data logging for off-line analysis of the navigational data.

The usage of the OpenIGTLink framework makes this work flexible. The developed windows client could be considered as a bridge from the Medtronic world to the open-source world: without any modification in fact the client could send navigational data to other software that supports OpenIGTLink. An example of another Medical visualization software (commercial) integrated with OpenIGTLink is MeVisLab[8]. There are also some commercial devices that have been integrated in a software library (IGSTK [11]) specifically designed

to provide the components of image-guided surgery (IGS) applications. Since OpenIGTLink is fully compatible with this library, other IGS devices could be easily integrated with the Medtronic navigator data.

6.1.1 Intra-operative usage

The integrated system showed its robustness in term of software stability during 7 surgical procedures that lasted from 3 to 8 hours. It has never been required to restart or reinitialize the communication from the Medtronic navigator to 3DSlicer. The testing of the system in some clinical situations during previous surgery has been necessary to adapt it to the surgical workflow and to define the acquisition protocol for the intraoperative points acquisition.

It is important to say that the system is not approved for clinical use. It has anyway been used clinically because it is only an additional system, and it does not influence the behavior of the Medtronic navigator.

6.1.2 Source Code management

The source code developed for this work is composed by two parts. The code of the Windows client (C++) and the code of the 3DSlicer module (python script). The first part has been already sent to Medtronic. The company is interested in making the code available to the scientific community after the code porting to the new version of StealthLink. The navigator module script too, will be shared with the Slicer community as soon as the windows client will be released by Medtronic.

6.2 Brain shift study

The reason leading the author to start this investigation has been the extent of the phenomena that could invalidate the reliability of a navigation system. The localization capability of a navigator is lost in case of brain shift phenomenon: a target identification error of about 5 mm might influence the surgery outcome by compromising the patient life. Neuronavigators should in fact be used with extremely caution by surgeons. Tying to measure and understand the brain shift problem could be the very first step to its possible solution.

One of the main weakness of the presented study is the **acquisition methodology**. The repositioning of the tool tip on the same target could be done only roughly by the surgeon. Nevertheless this error has been been inevitably incorporated in the brain shift measurement, but accurately discussed in section 5.3.1. The TRE used as a threshold for data reliability considers all the possible sources of error with this methodology. Necessarily this issue has reduced the number of available data for this study.

Another limitation is concerning the **timing** of acquisitions. In the phase immediately after the craniotomy it has not been possible to measure the shift that eventually occurred. As mentioned, the reference acquisition for the shift

analysis has been the first cortical acquisition. This acquisition was always been performed at least half an hour after the craniotomy acquisition (that corresponds to the beginning of the dura mater opening which requires at least half an hour.

Also the shift direction analysis showed some limitations: this study gives good results only when the shift vector has a module bigger than the defined threshold. The patients with brain shift smaller than TRE gives in fact **direction results not feasible**. The reasons are two:

1. when the shift vector has a module smaller than TRE its direction is not representative of the shift but it is only representative of the inaccurate repositioning of the pointer on the target during different acquisitions. Even accurate repositioning would always results in points with different coordinates, the nonzero vector between those points can not be considered for brain shift analysis;

2. Cortical points with opposite shift direction should be analyzed separately. This concepts is is clear in figure 4.11 and is confirmed by the big interquartile ranges in Figure 4.5.

Despite all these limitations, the proposed study gives some results aligned with the state of the art[27]. It has in fact being demonstrated that brain shift is mainly influenced by gravity. It has been shown instead how the inward direction (craniotomy normal) is not predominant. The evaluation of this direction was made in order to take into account the influence of the intracranial pressure decrease due to the intraoperative cerebrospinal fluid loss.

A correlation between the type of surgery has been found only qualitatively: from the 4 patients with significant brain shift (>TRE), the 2 patients with greater brain shift are the ones that underwent the deeper resection (lobectomies).

In conclusion the results found with this study are promising, but in order to be considered a clinical study for brain shift estimation future work should be done.

6.3 Future work

The implemented system opens a wide variety of future works. The work could move in different directions:

1. the optimization of the integration adding functions for improving the navigator usability also from a sterile user (the surgeon);

2. the continuation of the brain shift study with a larger number of patient observations (after the definition of acquisition protocol and results analysis that would improve the feasibility of the study);

3. the implementation of a system for automatic intraoperative model (exam) updating that would take as inputs the points acquired with the presented system;

4. performing different clinical study that would take advantage from the feature offered by the presented system.

For the first point some ideas have already been born:

- the navigated tool itself could be used as an input device for the Slicer scene, the implementations modality could be of two types:

    1. specific pointed locations would be codified as specific signals for the software
    2. specific gestures with the pointer (probe tip trajectories) are codified as specific input to the software.

- The acquisition of a point (annotation feature) should be done with the foot switch pression with a specific encoding. A single pression could be used instead for freezing the image in the currently navigated point.

For the second future direction a better understanding of the feasibility of a similar study with this set-up should be considered starting from the observations out of this work. Having the possibility to analyze a bigger number of patient could give clinical value to the study.

The third option is the most ambitious: several groups in the world are working for finding a solution for the brain shift issue, as mentioned in the state of the art [10] different solutions have been proposed. An overall study about the feasibility of each possible solution should be considered carefully.

A work on the last direction already started: a thesis project regarding the comparison between the intraoperative (DES) and preoperative(fMRI) brain mapping. A quantitative evaluation of the two techniques will be possible by intraoperative annotations placed using the dedicated feature of the developed system.

Bibliography

[1] J Lobo Antunes. Egas moniz and cerebral angiography. *Journal of Neurosurgery*, 40(4):427–432, 1974.

[2] Michel A Audette, Frank P Ferrie, and Terry M Peters. An algorithmic overview of surface registration techniques for medical imaging. *Medical Image Analysis*, 4(3):201–217, 2000.

[3] JW Belliveau, DN Kennedy, RC McKinstry, BR Buchbinder, RM Weisskoff, MS Cohen, JM Vevea, TJ Brady, and BR Rosen. Functional mapping of the human visual cortex by magnetic resonance imaging. *Science*, 254(5032):716–719, 1991.

[4] Svenja Borchers, Marc Himmelbach, Nikos Logothetis, and Hans-Otto Karnath. Direct electrical stimulation of human cortex - the gold standard for mapping brain functions? *Nature reviews. Neuroscience*, 13(1):63–70, January 2012.

[5] Anders M Dale, Bruce Fischl, and Martin I Sereno. Cortical surface-based analysis: I. segmentation and surface reconstruction. *Neuroimage*, 9(2):179–194, 1999.

[6] Walter E Dandy. Ventriculography following the injection of air into the cerebral ventricles. *Annals of surgery*, 68(1):5, 1918.

[7] Nicola D'Apuzzo and Michael Verius. 3d monitoring of the intraoperative brainshift by means of photogrammetry. In *Society of Photo-Optical Instrumentation Engineers (SPIE) Conference Series*, volume 6805, page 22, 2008.

[8] Jan Egger, Junichi Tokuda, Laurent Chauvin, Bernd Freisleben, Christopher Nimsky, Tina Kapur, and William Wells. Integration of the openigtlink network protocol for image-guided therapy with the medical platform mevislab. *The International Journal of Medical Robotics and Computer Assisted Surgery*, 2012.

[9] A. Fedorov, R. Beichel, J. Kalpathy-Cramer, J. Finet, J.C. Fillion-Robin, S. Pujol, C. Bauer, D. Jennings, F. Fennessy, M. Sonka, et al. 3d slicer as an

image computing platform for the quantitative imaging network. *Magnetic Resonance Imaging*, 2012.

[10] Matthieu Ferrant, Arya Nabavi, Benoit Macq, Ferenc A. Jolesz, Ron Kikinis, and Simon K. Warfield. Registration of 3-d intraoperative mr images of the brain using a finite-element biomechanical model. *Medical Imaging, IEEE Transactions on*, 20(12):1384–1397, 2001.

[11] Kevin Gary, Luis Ibanez, Stephen Aylward, David Gobbi, M Brian Blake, and Kevin Cleary. Igstk: an open source software toolkit for image-guided surgery. *Computer*, 39(4):46–53, 2006.

[12] P Grunert, K Darabi, J Espinosa, and R Filippi. Computer-aided navigation in neurosurgery. *Neurosurgical review*, 26(2):73–99, 2003.

[13] Marc Guenot, Jean Isnard, Philippe Ryvlin, Catherine Fischer, Karine Ostrowsky, Fran&ccedil ois Mauguiere, and Marc Sindou. Neurophysiological monitoring for epilepsy surgery: the talairach seeg method. *Stereotactic and functional neurosurgery*, 77(1-4):29–32, 2002.

[14] Tamas Haidegger, Tian Xia, and Peter Kazanzides. Accuracy improvement of a neurosurgical robot system. *2008 2nd IEEE RAS & EMBS International Conference on Biomedical Robotics and Biomechatronics*, pages 836–841, October 2008.

[15] Fei Li, Jiangkai Lin, Gang Zhu, Hui Meng, Nan Wu, Rong Hu, and Hua Feng. Neuroimaging and functional navigation as potential tools to reduce the incidence of surgical complications of lateral ventricular meningiomas. *Clinical neurology and neurosurgery*, 113(7):564–9, September 2011.

[16] Christopher R Mascott. Comparison of magnetic tracking and optical tracking by simultaneous use of two independent frameless stereotactic systems. *Neurosurgery*, 57(4):295–301, 2005.

[17] Christopher R Mascott. In vivo accuracy of image guidance performed using optical tracking and optimized registration. *Journal of neurosurgery*, 105(4):561–567, 2006.

[18] M I Miga, K D Paulsen, J M Lemery, S D Eisner, a Hartov, F E Kennedy, and D W Roberts. Model-updated image guidance: initial clinical experiences with gravity-induced brain deformation. *IEEE transactions on medical imaging*, 18(10):866–74, October 1999.

[19] Michael Miga, Keith Paulsen, Francis Kennedy, Jack Hoopes, Alex Hartov, and David Roberts. Initial in-vivo analysis of 3d heterogeneous brain computations for model-updated image-guided neurosurgery. In *Medical Image Computing and Computer-Assisted InterventationMICCAI98*, pages 743–752. Springer, 1998.

[20] Herke J. Noordmans, Peter a. Woerdeman, Peter W. a. Willems, Peter C. van Rijen, and Jan W. Berkelbach van der Sprenkel. Sound and volumetric workflow feedback during image guided neurosurgery. *Proceedings of SPIE*, 6842:68422J–68422J–9, 2008.

[21] Daniel a Orringer, Alexandra Golby, and Ferenc Jolesz. Neuronavigation in the surgical management of brain tumors: current and future trends. *Expert review of medical devices*, 9(5):491–500, September 2012.

[22] X Papademetris, KP Vives, M DiStasio, LH Staib, M Neff, S Flossman, N Frielinghaus, H Zaveri, EJ Novotny, H Blumenfeld, et al. Development of a research interface for image guided intervention: Initial application to epilepsy neurosurgery. In *Biomedical Imaging: Nano to Macro, 2006. 3rd IEEE International Symposium on*, pages 490–493. IEEE, 2006.

[23] Xenophon Papademetris, Marcel Jackowski, Nallakkandi Rajeevan, Marcello DiStasio, Hirohito Okuda, R Todd Constable, and Lawrence H Staib. Bioimage suite: An integrated medical image analysis suite: An update. *Computer software]. Available from http://www. bioimagesuite. org*, 2006.

[24] Sujit S Prabhu, Jaime Gasco, Sudhakar Tummala, Jefrey S Weinberg, and Ganesh Rao. Intraoperative magnetic resonance imaging-guided tractography with integrated monopolar subcortical functional mapping for resection of brain tumors. *Journal of neurosurgery*, 114(3):719–726, 2011.

[25] Paul R Rider. On the distribution of the correlation coefficient in small samples. *Biometrika*, 24(3/4):382–403, 1932.

[26] D W Roberts, a Hartov, F E Kennedy, M I Miga, and K D Paulsen. Intraoperative brain shift and deformation: a quantitative analysis of cortical displacement in 28 cases. *Neurosurgery*, 43(4):749–58; discussion 758–60, October 1998.

[27] D.W. Roberts, A. Hartov, F.E. Kennedy, M.I. Miga, and K.D. Paulsen. Intraoperative brain shift and deformation: a quantitative analysis of cortical displacement in 28 cases. *Neurosurgery*, 43(4):749–758, 1998.

[28] Andrea Romano, Giancarlo D'Andrea, Luigi Fausto Calabria, Valeria Coppola, Camilla Rossi Espagnet, Alberto Pierallini, Luigi Ferrante, Luigi Fantozzi, and Alessandro Bozzao. Pre-and intraoperative tractographic evaluation of corticospinal tract shift. *Neurosurgery*, 69(3):696–705, 2011.

[29] Reuben R Shamir, Leo Joskowicz, Sergey Spektor, and Yigal Shoshan. Localization and registration accuracy in image guided neurosurgery: a clinical study. *International journal of computer assisted radiology and surgery*, 4(1):45–52, January 2009.

[30] Medtronic Computer-Assisted Surgery Systems. Stealthlink instructions.

[31] Junichi Tokuda, S Gregory, Ziv Yaniv, Patrick Cheng, Jack Blevins, Alexandra J Golby, Tina Kapur, Steve Pieper, and Everette C Burdette. OpenIGTLink : an open network protocol for image-guided therapy environment. (May):423–434, 2009.

[32] Jay B West, J Michael Fitzpatrick, Steven A Toms, Calvin R Maurer Jr, and Robert J Maciunas. Fiducial point placement and the accuracy of point-based, rigid body registration. *Neurosurgery*, 48(4):810–817, 2001.

[33] Gerlig Widmann, Peter Schullian, Martin Ortler, and Reto Bale. Frameless stereotactic targeting devices: technical features, targeting errors and clinical results. *The International Journal of Medical Robotics and Computer Assisted Surgery*, 2011.

[34] Jin-Song Wu, Liang-Fu Zhou, Wei-Jun Tang, Ying Mao, Jin Hu, Yan-Yan Song, Xun-Ning Hong, and Gu-Hong Du. Clinical evaluation and follow-up outcome of diffusion tensor imaging-based functional neuronavigation: a prospective, controlled study in patients with gliomas involving pyramidal tracts. *Neurosurgery*, 61(5):935–949, 2007.

[35] Amir Zolal, Aleš Hejcl, Petr Vachata, Robert Bartoš, Ivan Humhej, Alberto Malucelli, Martina Nováková, Karel Hrach, Milouš Derner, and Martin Sameš. The use of diffusion tensor images of the corticospinal tract in intrinsic brain tumor surgery: A comparison with direct subcortical stimulation. *Neurosurgery*, 71(2):331–340, 2012.